



## ORIGINAL PAPER

**UNCERTAINTY QUANTIFICATION IN THE ANALYSIS OF LIQUEFIED SOIL RESPONSE THROUGH FUZZY FINITE ELEMENT METHOD**

Farhoud KALATEH \*, Farideh HOSSEINEJAD \* and Milad KHEIRY

Faculty of Civil Engineering, University of Tabriz, P.O. Box, 51666-16471 Tabriz, Iran

\*Corresponding author's e-mail: [fkalateh@tabrizu.ac.ir](mailto:fkalateh@tabrizu.ac.ir); [f.hosseinejad@tabrizu.ac.ir](mailto:f.hosseinejad@tabrizu.ac.ir)**ARTICLE INFO****Article history:**

Received 20 December 2021

Accepted 30 May 2022

Available online 14 June 2022

**Keywords:**

Fuzzy finite element

Liquefaction

Coupled hydro-mechanical equations

Membership function

Uncertainty quantification

**ABSTRACT**

In the present study, a scheme based on fuzzy finite element method was provided for uncertainty quantification of liquefied saturated soil response under dynamic loading. In this respect, the coupled dynamic equations which are known as u-p equations were used, and instead of crisp values for input parameters, including permeability coefficient, specific mass of the soil, compressibility and shear modulus, their fuzzy numbers were used. At the end, displacements and pore water pressure created during earthquake were reported as fuzzy numbers. After verifying procedures of fuzzy analysis by experimental results from the centrifuge model test No. 1 from the VELACS project, several membership grades were considered. Firstly, the effect of fuzzification of each input soil parameter investigated individually, and then effect of considering all four input soil parameters as fuzzy numbers was analyzed by developed method. It was indicated that results of the analysis during the effective time of the earthquake were strongly influenced by the shear modulus and partially by compressibility modulus, and after this time, it was mainly affected by the permeability coefficient. Also considering uncertainty nature of specific mass of the soil had no significant effect on the results.

**1. INTRODUCTION**

Soil liquefaction appears to be particularly easily affected by heterogeneity and randomness of soil properties (Popescu and Prevost, 1995). Different studies have shown that both the expansion and the pattern of pore water pressure build-up in saturated soil subjected to seismic excitation are different when computed by stochastic simulation methods and when computed by deterministic numerical analyses, which use average values (Popescu and Prevost, 1995; Ohtomo and Shinozuka, 1990; Fenton, 1990; Ural, 1995; Popescu et al., 1997; Fenton and Griffith, 2008). So, in the present research, for quantify the uncertainty effects that interwoven with soil properties in the assessment of liquefied soil response a scheme based on fuzzy finite element is provided and detailed investigated. The deterministic Finite Element (FE) method is an efficient tool to accurately solve the Partial Differential Equations (PDE) that govern most real-world problems; but it considers only average values for the input parameters, obtained from some experimental data set. According to this procedure, the output value is unique, which is not able to accurately express the uncertainties related to the input parameters and their inherent variability (Silva et al., 2016). So it is enhanced by integrating model parameter uncertainty into FE model (Faes et al.,

2017). Source of uncertainty is incomplete information resulting from vagueness, non-specificity or dissonance. Vagueness characterizes information which is imprecisely defined, unclear or indistinct. It is typically the result of human opinion on unknown quantities (Farkas et al., 2010). According to source of uncertainty, two approaches of probability and possibility theories are adopted to solve it mathematically. Probabilistic concepts have been introduced for non-deterministic numerical modeling. Stochastic finite element method (SFEM) is one of the powerful numerical methods as previously used appropriately for considering random characteristics of soil properties in different geotechnical problems such as liquefaction analysis (Popescu and Prevost, 1995; Ohtomo and Shinozuka, 1990; Fenton, 1990; Ural, 1995; Popescu et al., 1997; Fenton and Griffith, 2008) but the main obstacle to use this method is being costly and time consuming specially when this method combined with Monte Carlo simulation method. In this regards, interval and fuzzy approaches are becoming increasingly popular for the analysis of numerical models, such as fuzzy finite element method (FFEM), that incorporate uncertainty in their description (Faybishenko, 2010) despite its simplicity and straightforwardness the obtained results are acceptable and accurate. In the interval approach, the

uncertainty is modelled as two crisp bounds on the variable between which all possible values lie, and thus propagated. So for each uncertainty, the analyst has to provide the lower and upper bound. The fuzzy approach extends this methodology by introducing a level of membership that represents to what extent a certain value is member of the range of possible input values. The membership of a variable to an interval is considered as a continuous function, ranging from 0 to 1. Membership grade of  $\alpha = 0$  indicates the variable is certainly no part of the interval and membership grade of  $\alpha = 1$  insures the variable lies in the interval (Farkas et al., 2010; Meidani et al., 2004). This concept provides the analyst with a tool to express a degree of possibility for a certain value. Based on the  $\alpha$  sub level technique, the fuzzy analysis requires the consecutive solution of a number of related interval problems (Moens and Hanss, 2011). The imprecise characteristic of soil properties has encouraged application of fuzzy sets in geotechnical engineering instead of using probabilistic methods that have still remain a mystery to engineers and underestimated the results in some cases (Silva et al., 2016). The theory of fuzzy sets is generally regarded as the most effective tool for processing qualitative information and inexact data. As stated, If the form of uncertainty happens to arise because of imprecision, ambiguity, or vagueness, then the variable is probably fuzzy and can be represented by a membership function (Li and Lumb, 1987). So, all soil parameters having uncertainty may be defined as fuzzy numbers (Meidani et al., 2004). Fuzzy calculations can be performed by the analytical extension principle (Zadeh, 1999), or a numerical method such as the vertex method (Dong and Shah, 1987), and the DSW algorithm (Dong et al., 1985). In the current study a numerical scheme base on fuzzy finite element method (FFEM) is provided and applied to soil liquefaction problem and present the ability of FFEM in the investigated the probabilistic quantification of this complex problem. In this respect, coupled hydro mechanical equations (Biot, 1941; Biot, 1956; Biot, 1962; Zienkiewicz and Bettess, 1982; Zienkiewicz and Shiomi, 1984; Zienkiewicz et al., 1990) govern to saturated porous media were solved through fuzzy finite element method (FFEM). Uncertainty of soil properties were included by assuming of soil specific mass, permeability coefficient, compressibility and shear modulus as fuzzy input parameters. In our previous work (Hosseinejad and Kalateh, 2017) soil was considered elastic but in current study, Pastor- III model (Pastor et al., 1990) was applied to considered nonlinear behavior of soil during liquefaction. Pastor-III model was used widely for dynamic analysis of porous medium in recent years (Khoei et al., 2011a; Khoei et al., 2004; Khoei et al., 2011b; Rahmani et al., 2012; Sadeghian and Namin, 2013; Tamayo and Awruch, 2016; Hosseinejad et al., 2019).

## 2. FUZZY SETS

Fuzzy set is defined as a class of objects with a continuum of membership grades between the values of zero to one. A fuzzy set allows a gradual change from one class to another instead of an abrupt boundary as in an ordinary set. If  $M$  is considered as a universe set, set of  $A$  will be a fuzzy subset of  $M$ . It can be written as a set of ordered pairs as follows:

$$A = \{[m, \mu_A(m)], m \in M\} \quad (1)$$

where  $\mu_A(m)$  is called membership grade of  $m$  and has a value in the closed interval of  $[0,1]$ . If  $[0, 1]$  is replaced by two-element set of  $\{0, 1\}$ , then  $A$  can be regarded as an ordinary subset of  $M$ . For the sake of simplicity, thenotion fuzzy set is utilized instead of fuzzy subset. Particular case of fuzzy sets is fuzzy numbers. A fuzzy number such as  $A$  is a vertices subset of real numbers, which means a, b, c with,  $a < c < b$  for every real number (McBratney and Odeh, 1997):

$$\mu_A(c) \geq \min(\mu_A(a), \mu_A(b)) \quad (2)$$

It indicates that membership function of a fuzzy number consists of increasing and decreasing parts and there is only one member of the series such as  $z$  with a membership grade equals to one ( $\mu_A(z) = 1$ ). Each fuzzy number is determined by its support, which is set as follows:

$$\text{supp}(A) = \{x, \mu_A(x) > 0\} \quad (3)$$

Convexity assumption (Eq. (2)) ensures that the support of fuzzy number is an interval. And the membership grade of a real number, represents the probability of its occurrence. Among Fuzzy calculation methods, vertex method (Dong and Shah, 1987) simplifies manipulations of the extension principle for continuous-valued fuzzy variables. It can prevent abnormality in the output membership function due to application of the discretization technique on the domain of the fuzzy variables. Also it can prevent the widening of the resulting function value set due to multiple occurrences of variables in the functional expression by conventional interval analysis methods (Ross, 2004). Suppose we have a single-input mapping given by  $y = f(x)$  that is to be extended for fuzzy sets, or  $B = f(A)$ , and we want to decompose  $A$  into a series of  $\lambda$ -cut intervals, say  $I_\lambda$  ( $\lambda = 0+ to \lambda = 1$ ). When the function  $f(x)$  is continuous and monotonic on  $I_\lambda = [a, b]$ , the interval representing  $B$  at a particular value of  $\lambda$ , say  $B_\lambda$ , can be obtained as (Ross, 2004):

$$B_\lambda = f(I_\lambda) = [\min(f(a), f(b)), \max(f(a), f(b))] \quad (4)$$

Otherwise, when the function  $f(x)$  is not monotonic and its extreme points exist in the  $n$ -dimensional Cartesian region of the input parameters,  $B_\lambda$  is defined as

$$B_\lambda = f(I_\lambda) = [\min(f(c_i), f(E_j)), \max(f(c_i), f(E_j))] \quad (5)$$

where  $c_i$  is the coordinate of the  $i$ th vertex representing the  $n$ -dimensional Cartesian region.  $i = 1, 2, \dots, N$  and  $j = 1, 2, \dots, m$ .  $m$  is number of extreme points in the region.

### 2.1. MEMBERSHIP FUNCTION

A fuzzy number is defined by membership function of  $\mu(x)$  and membership function is formed in various ways. Improved linear triangular membership function, which was introduced by (Valliappan and Pham, 1993, 1995) and to consider opinion of expert is illustrated in Figure 1 and defined as follows:

$$\mu(x) = \begin{cases} 0, & x \leq l' \\ \frac{x-l'}{m-l'}, & l' \leq x \leq m \\ \frac{h'-x}{h'-m}, & m \leq x \leq h' \\ 0, & x \geq h' \end{cases} \quad (6)$$

where

$$l' = \begin{cases} m - 2(m - l), & m \geq 2(m - l) \\ 0, & m \leq 2(m - l) \end{cases} \quad (7)$$

$$h' = m + 2(h - m) \quad (8)$$

$l$ ,  $m$  and  $h$  are most likely expert's estimates for low and high values of a parameter and  $l'$  and  $h'$  are the extreme low and high values of parameters of  $l$  and  $h$  respectively.

In the present study, it is supposed that the dynamic coupled analysis is implemented to input uncertainties including the soil permeability  $K$ , specific mass of the soil  $\rho$ ,  $kev$  bulk modulus at mean effective stress of soil and  $kes$  a model parameter (three times the shear modulus at mean effective stress), with the crisp values  $K_c, \rho_c, kev_c$  and  $kes_c$  (Fig. 1a) and support ends hydro-mechanical coupled dynamic systems the liquefied response of soil media, i.e. nodal displacements and pore water pressure, become uncertain too.

With introducing a  $\alpha$ -cut operator to each fuzzy number the continues membership function is discretized into several discrete levels as shown in Figure 2b. At cut  $\alpha = 0$  the variables have the highest uncertainty while at cut  $\alpha = 1$  the variables have exactly their crisp values. To assess the fussy responses at the level of membership function  $\mu$  (the level of uncertainty), first the  $\alpha$ -cut operator with  $[K^{a,\alpha}, K^{b,\alpha}]$ ,  $[\rho^{a,\alpha}, \rho^{b,\alpha}]$ ,  $[kev^{a,\alpha}, kev^{b,\alpha}]$  and  $[kes^{a,\alpha}, kes^{b,\alpha}]$  is introduced to input fuzzy numbers. As shown in Figure 1c, when the input variables are cut by certain  $\alpha$ ,  $d_i$  and  $p_i$  the nodal soil displacements and nodal pore water pressures in the time history are obtained at the same level of membership functions as intervals  $[d_i^{a,\alpha}, d_i^{b,\alpha}]$  and  $[p_i^{a,\alpha}, p_i^{b,\alpha}]$ , respectively. Whit applying different

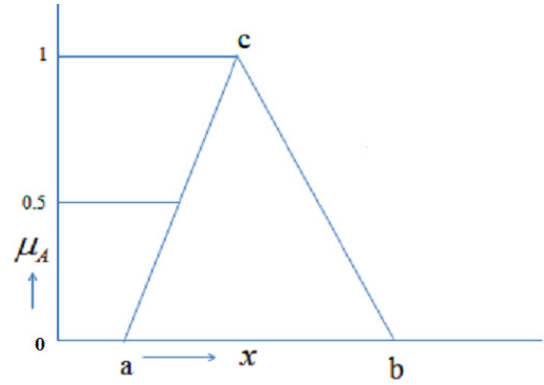


Fig. 1 Definition of triangular fuzzy number  $[a,c,b]$ .

levels of  $\alpha$ -cut operators (from  $\alpha = 0$  to 1) one can obtain the shape of membership function of each response of interest.

### 3. MATHEMATICAL MODEL FOR INTERACTION OF PORE FLUID FLOW AND SOIL SKELETON

Governing equations for saturated porous medium with a single fluid phase, generally water, are formulated based on total equilibrium of soil-pore fluid mixture, mass balance of flow equation, concept of effective stress, constitutive model for soil behavior, and equilibrium equation for pore fluid which is called generalized Darcy's equation. Final governing equations of saturated porous medium, involve two variables of  $u$  and  $p$  are as follows. Details on these equations are given in (Khoei et al., 2004).

$$\sigma_{ij,j} + \rho \ddot{u}_i - \rho b_i = 0 \quad (9)$$

$$[K_{ij}(p_{,j} + \rho_f \ddot{u}_j - \rho_f b_j)]_{,i} + \alpha \dot{\epsilon}_{ii} + \frac{p}{C} = 0 \quad (10)$$

where  $\sigma_{ij}$  is total stress and according to the effective stress principle it is defined as  $\sigma_{ij} = \sigma'_{ij} + \delta_{ij} n p$  by  $\delta_{ij}$  and  $n$  denoting Kronecker delta and porosity respectively (Zienkiewicz et al., 1999)  $u$  is displacement vector of soil skeleton and  $p$  is pore pressure.  $b_i$  is body force per unit mass,  $\rho_f$  is fluid density and  $\rho$  is the density of total composite which is defined by  $\rho = n \rho_f + (1 - n) \rho_s$ , in which  $\rho_s$  is the density of solid particles.  $K_{ij}$  is permeability per unit weight,  $\epsilon_{ij}$  are total strains and  $C$  is combined compressibility which is defined as  $C = \frac{n}{k_f} + \frac{(1-n)}{k_s}$ .  $k_s$

denotes bulk modulus of solid particles and  $k_f$  bulk modulus of fluid.  $\alpha$  is dependent upon material type and is taken to be unite for soils. Equations (9) and (10) together form the u-p formulation, which must necessitate the solution in a coupled manner. Replacing variables  $u$  and  $p$  with  $u = \sum N_i^u u_i = N^u \bar{u}$  and  $p = \sum N_i^p p_i = N^p \bar{p}$  then multiplying equation (9) by  $(N^p)^T$  and equation (10) by  $(N^u)^T$ , finally integrating over the domain, discrete form of coupled equation can be obtained as follows (Ye et al., 2013; Hosseinejad et al., 2019):

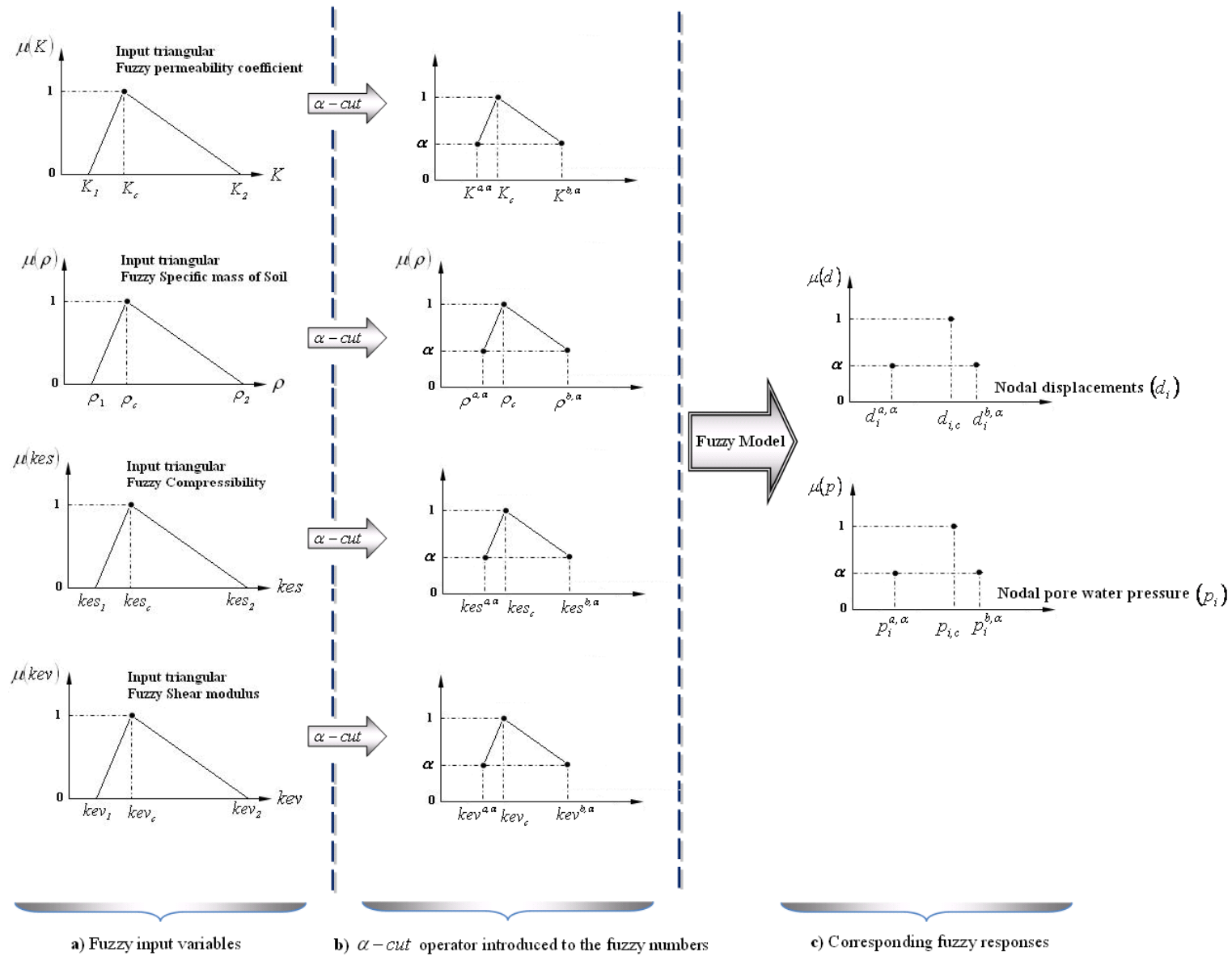


Fig. 2 The fuzzy input-output model.

$$\begin{bmatrix} [M]_{n+1} + \frac{1}{2}\beta_2\Delta t^2[k_m]_{n+1} & -\Delta t\theta[Q]_{n+1} \\ \beta_1\Delta t[Q]_{n+1}^T & [S]_{n+1} + \Delta t\theta[k_c]_{n+1} \end{bmatrix} \begin{Bmatrix} \{\Delta\ddot{u}_n\} \\ \{\Delta\dot{p}_n\} \end{Bmatrix} = \begin{Bmatrix} \{f^1\}_{n+1} - \{f^1\}_n + [Q]_{n+1}\{\dot{p}_n\}\Delta t - [k_m]_{n+1}(\{\dot{u}_n\}\Delta t + \frac{1}{2}\{\ddot{u}_n\}\Delta t^2) \\ \{f^2\}_{n+1} - \{f^2\}_n - [k_c]_{n+1}\{\dot{p}_n\}\Delta t - [Q]_{n+1}\{\ddot{u}_n\}\Delta t \end{Bmatrix} \quad (11)$$

where  $\Delta t$  is the step.  $\beta_1$ ,  $\beta_2$  and  $\theta$  are integration constants used in Newmark scheme. Parameters of acceleration, velocity, displacement, pore pressure at time  $t^{n+1}$  will be as follows (Khoei et al., 2004; Zienkiewicz et al., 1999; Ye et al., 2013; Hosseinejad et al., 2019).

$$\ddot{u}_{n+1} = \ddot{u}_n + \Delta\ddot{u}_n \quad (12a)$$

$$\dot{u}_{n+1} = \dot{u}_n + \ddot{u}_n\Delta t + \beta_1\Delta\ddot{u}_n\Delta t \quad (12b)$$

$$\bar{u}_{n+1} = \bar{u}_n + \dot{u}_n\Delta t + \frac{1}{2}\ddot{u}_n\Delta t^2 + \frac{1}{2}\beta_2\Delta\ddot{u}_n\Delta t^2 \quad (12c)$$

$$\dot{p}_{n+1} = \dot{p}_n + \Delta\dot{p}_n \quad (12d)$$

$$p_{n+1} = p_n + \dot{p}_n\Delta t + \theta\Delta\dot{p}_n\Delta t \quad (12e)$$

In this study,  $\beta_1 = 0.6$ ,  $\beta_2 = 0.605$  and  $\theta = 0.6$  are employed (Zienkiewicz et al., 1999; Ye et al., 2013).  $M$ ,  $K_m$ ,  $Q$ ,  $S$ , and  $k_c$  are the mass, stiffness, coupling, compressibility and permeability matrixes respectively.  $f^{(1)}$  and  $f^{(2)}$  are nodal force vectors. They are expressed as follows (Khoei et al., 2004; Zienkiewicz et al., 1999; Ye et al., 2013):

$$[M] = \int (N^u)^T \rho N^u d\Omega \quad (13a)$$

$$[k_m] = \int [B]^T [D] [B] d\Omega \quad (13b)$$

$$[Q] = \int [B]^T S_w m [N^p] d\Omega \quad (13c)$$

$$[k_c] = \int [B_p]^T [\kappa] [B_p] d\Omega \quad (13d)$$

$$[S] = \int N^p \left(\frac{1}{c}\right) N^p d\Omega \quad (13e)$$

$$B = \begin{bmatrix} \frac{\partial N_1^u}{\partial x} & 0 & \dots & \frac{\partial N_8^u}{\partial x} & 0 \\ 0 & \frac{\partial N_1^u}{\partial y} & \dots & 0 & \frac{\partial N_8^u}{\partial y} \\ \frac{\partial N_1^u}{\partial y} & \frac{\partial N_1^u}{\partial x} & \dots & \frac{\partial N_8^u}{\partial y} & \frac{\partial N_8^u}{\partial x} \end{bmatrix} \quad (13f)$$

$$B_p = \begin{bmatrix} \frac{\partial N_1^p}{\partial x} & \frac{\partial N_2^p}{\partial x} & \dots & \frac{\partial N_4^p}{\partial x} \\ \frac{\partial N_1^p}{\partial y} & \frac{\partial N_2^p}{\partial y} & \dots & \frac{\partial N_4^p}{\partial y} \end{bmatrix} \quad (13i)$$

$$f^{(1)} = \int [N^u]^T \rho b d\Omega + \int_r [N^u]^T \bar{t} d\Gamma \quad (13j)$$

$$f^{(2)} = - \int [N^p]^T \nabla^T (k S_w \rho_f b) d\Omega + \int_r [N^p]^T \bar{q} d\Gamma \quad (13h)$$

where  $m$  is a vector written as  $\mathbf{m}=[1, 1, 1, 0, 0, 0]^T$  in general and  $\mathbf{m}=[1, 1, 0]^T$  in plan strain conditions.  $\bar{t}$  is the stress and  $\bar{q}$  is the water flux acting on the surface of the computational domain.  $\kappa$  is permeability. In elastic soil model  $D$  can be expressed as:

$$D = \frac{E}{(1+\nu)(1-2\nu)} \begin{bmatrix} 1-\nu & \nu & 0 \\ \nu & 1-\nu & 0 \\ 0 & 0 & \frac{1-2\nu}{2} \end{bmatrix} \quad (14)$$

where  $E$  is the elastic modulus and  $\nu$  is Poisson's ratio of soil, that can be defined as

$$\nu = \frac{3kev-2G}{6kev+2G}, E = 3kev(1-2\nu), G = \frac{kes}{3} \quad (14a)$$

where  $kev$  is bulk modulus at mean effective stress of soil and  $kes$  is a model parameter (three times the shear modulus at mean effective stress) and  $G$  is shear modulus. In elasto-plastic soil model such as PZIII (Pastor et al.,

1990), the elastic matrix  $\mathbf{D}$  should be replaced by the elastoplastic matrix  $\mathbf{D}^{ep}$  (Ye et al., 2013):

$$\mathbf{D}^{ep} = \mathbf{D}^e - \frac{D^e m n D^e}{H_{L/U} + n D^e m} \quad (15)$$

where  $D^e$  is the elastic stiffness tensor,  $H_{L/U}$  is the plastic modulus during loading/unloading,  $m$  is the plasticflow direction vector, and  $n$  is the loading or unloading direction vector (Zienkiewicz et al., 1999). Here  $L$  and  $U$  denote the corresponding quantities for loading and unloading, respectively. In PZIII model, there is no need to explicitly define yield and plastic potential surfaces, because  $m$  and  $n$  are defined as (Chan, 1988):

$$m = (m_v, m_s, m_\theta) = \frac{(d_g, 1, \frac{q}{2} M_g \cos 3\theta)}{\sqrt{1+d_g^2}} \quad (16)$$

$$n = (n_v, n_s, n_\theta) = \frac{(d_f, 1, \frac{q}{2} M_f \cos 3\theta)}{\sqrt{1+d_f^2}} \quad (17)$$

$$d_g = (1 + \alpha_g) \cdot (M_g - \eta) \quad (18)$$

$$d_f = (1 + \alpha_f) \cdot (M_f - \eta) \quad (19)$$

where  $\alpha_g$  and  $\alpha_f$  are model parameters.  $M_g$  is the gradient of the critical state line in the  $p$ - $q$  plane. Generalizing  $M_g$  to the three-dimensional stress conditions and modifications of the Mohr-Coulomb type results in (Chan, 1988):

$$M_g = \frac{6 \sin \phi_g}{3 - \sin \phi_g \cdot \sin 3\theta} \quad (20)$$

where  $\phi_g$  is the remaining friction angle in the tri axial test and  $\theta$  is Lode angle defined as:

$$\theta = \frac{1}{3} \sin^{-1} \left( -\frac{3\sqrt{3}}{2} \cdot \frac{j_3}{j_2^2} \right) \quad (21)$$

where  $M_f$  is the stress ratio at failure (Cen et al., 2018) and  $M_g/M_f$  is equal to relative density. Defining  $\hat{p} = \frac{j_1}{3}$  and  $q = \sqrt{3j_2}$ ,  $\eta = \frac{q}{\hat{p}}$  is stress ratio. The hardening rule is associated if  $d_f = d_g$ .  $H_L$  is the plastic modulus for the loading conditions and can be defined as:

$$\mathbf{H}_L = \mathbf{H}_0 \cdot \mathbf{p} \cdot \mathbf{H}_f \cdot \{ \mathbf{H}_v + \mathbf{H}_s \} \mathbf{H}_{DM} \quad (22a)$$

$$\mathbf{H}_f = \left( \mathbf{1} - \frac{\eta}{M_f} \cdot \frac{\alpha_f}{1+\alpha_f} \right)^4 \quad (22b)$$

$$\mathbf{H}_v = \mathbf{1} - \frac{\eta}{M_g} \quad (22c)$$

$$\mathbf{H}_s = \beta_0 \cdot \beta_1 \cdot \exp(-\beta_0 \xi) \quad (22d)$$

$$\mathbf{H}_{DM} = \left( \frac{\zeta_{max}}{\zeta} \right)^\gamma \quad (22e)$$

$$\xi = \int |d\epsilon_s^p| = \int d\xi \quad (22f)$$

$$\zeta = p \left\{ 1 - \left( \frac{\alpha_f}{1+\alpha_f} \right) \cdot \frac{\eta}{M_f} \right\}^{-1/\alpha_f} \quad (22g)$$

where  $H_0, \beta_0, \beta_1, \gamma$  are model parameters,  $\xi$  is the cumulative deviatoric plastic strain.  $\zeta$  is called the mobilized stress function and  $\zeta_{max}$  is the maximum value previously reached by the mobilized stress function. The plastic modulus obtained from Eq. (22a) can model some characteristics of the behavior of granular soils such as rupture in critical condition, softening of sands, and non-swelling (dilatation) of loose sand. For  $H_v + H_s > 0 (H_L > 0)$ , hardening of the material occurs, and for  $H_v + H_s < 0 (H_L < 0)$ , softening of the material occurs (Cen et al., 2018). In the case of unloading, the plastic modulus,  $H_U$  is also defined as follows:

$$\mathbf{H}_U = \mathbf{H}_{u0} \left( \frac{M_g}{\eta_u} \right)^{\gamma_u} \text{ for } \left| \frac{M_g}{\eta_u} \right| > 1 \quad (23a)$$

$$\mathbf{H}_U = \mathbf{H}_{u0} \text{ for } \left| \frac{M_g}{\eta_u} \right| \leq 1 \quad (23b)$$

where  $\gamma_u, H_{u0}$  are model parameters and  $\eta_u$  is the stress ratio at which the unloading occurred. In the pastor - Zienkiewicz model, the soil is assumed to has the nonlinear elastic response, and reversible nonlinear behavior is expressed by a hypo-elastic approach, in which the compressibility and shear modulus depend only on the hydrostatic pressure, and they are expressed as follows:

$$K = K_0 \frac{p}{p_0} \quad (24a)$$

$$G = G_0 \frac{p}{p_0} \quad (24b)$$

where  $p_0$  is a hydrostatic pressure in which the model parameters are measured and  $K_0$  and  $G_0$  are the initial values of the shear and compressibility modulus, respectively (Mira et al., 2009). The structure chart for incremental form of Biot analysis with fuzzy finite element method is illustrated in Figure 3.

#### 4. NUMERICAL SIMULATION RESULTS

Numerical example of elastic soil column was presented in order to illustrate the application of fuzzy finite element method in the dynamic analysis of deformable porous medium. For this purpose, soil properties are considered as fuzzy numbers according to data presented in Table 1. These input fuzzy numbers were depicted in Figure 4. In order to validate

**Table 1** Fuzzy material properties of soil column.

Parameters		Value
Kev(kPa)	l*	308
	m**	770
	h***	1232
Kes(kPa)	l	462
	m	1155
	h	1848
$\rho_s$ (kg/m <sup>3</sup> )	l	1.4035
	m	2.005
	h	2.6065
$\frac{k}{\gamma}$ (m <sup>3</sup> s/kg)	l	1.32e-4
	m	3.3 e-4
	h	5.28e-4

\*the least amount, \*\*the most likely value and \*\*\* the maximum value of the parameters

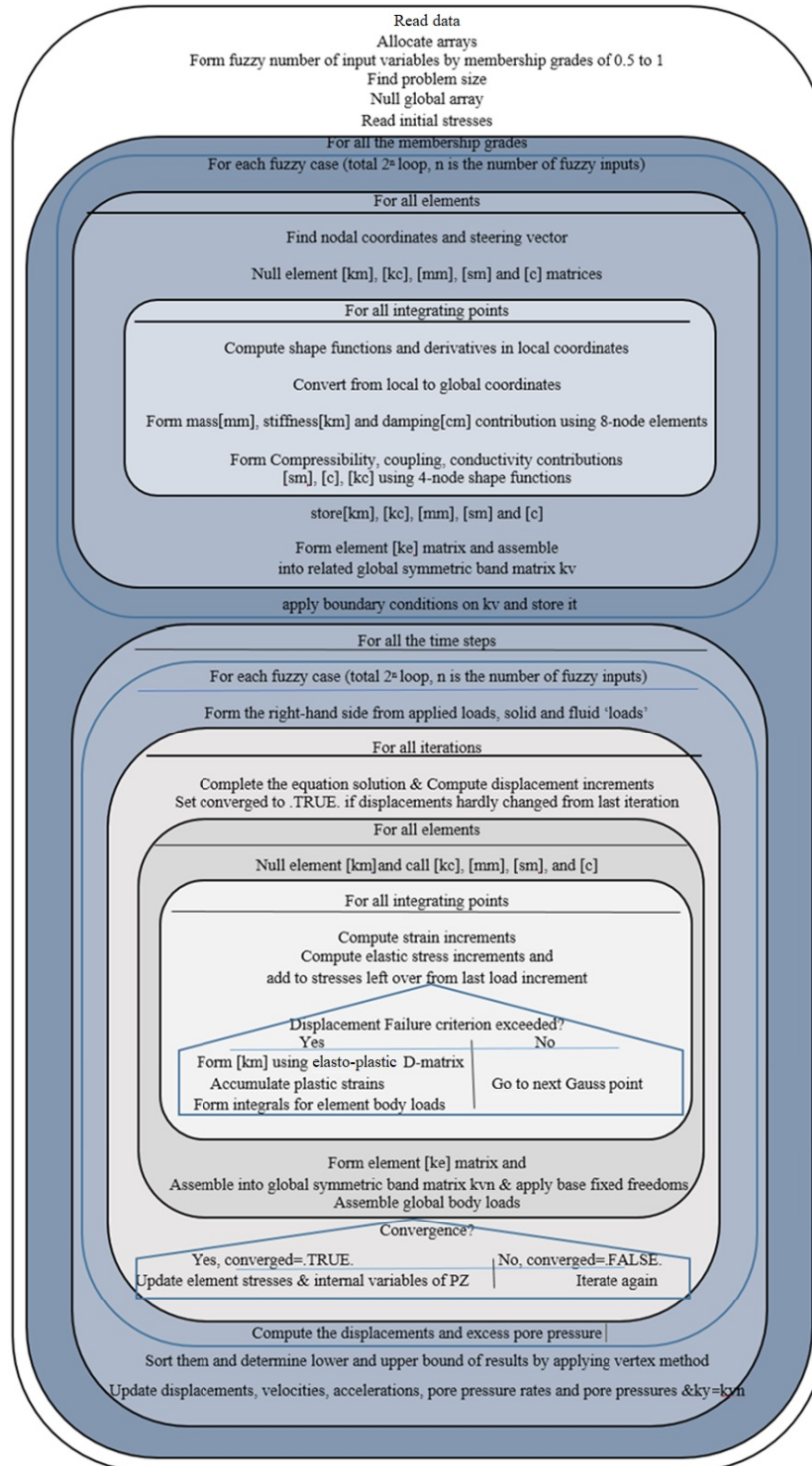


Fig. 3 Flow chart of developed FORTRAN code.

the developed numerical model, core of input fuzzy numbers was considered according to (Chan et al., 1993) with reference to the CIUC4051 and CY40115 experimental results obtained from (Arulmoli et al., 1992) who provided the standard soil model test results for numerical predictions. So the results obtained from the centrifuge model test No. 1 of VELACS (Verification of Numerical Procedures for the Analysis of Soil Liquefaction Problems) project, conducted by (Taboada and Dobry, 1993),

were used to demonstrate the capability of the numerical model for reliable analysis of the dynamic response. The sketch of the laminar box (prototype) and the instrumentation used for this experiment are shown in Figure 5 and Table 2. In the centrifuge test No. 1 of VELACS project, the soil profile contains a uniform horizontal layer of Nevada loose sand with a relative density of approximately 40 %. The soil layer (model) with a height of 0.2 m (10 m in the prototype scale) is placed into a laminar box. The

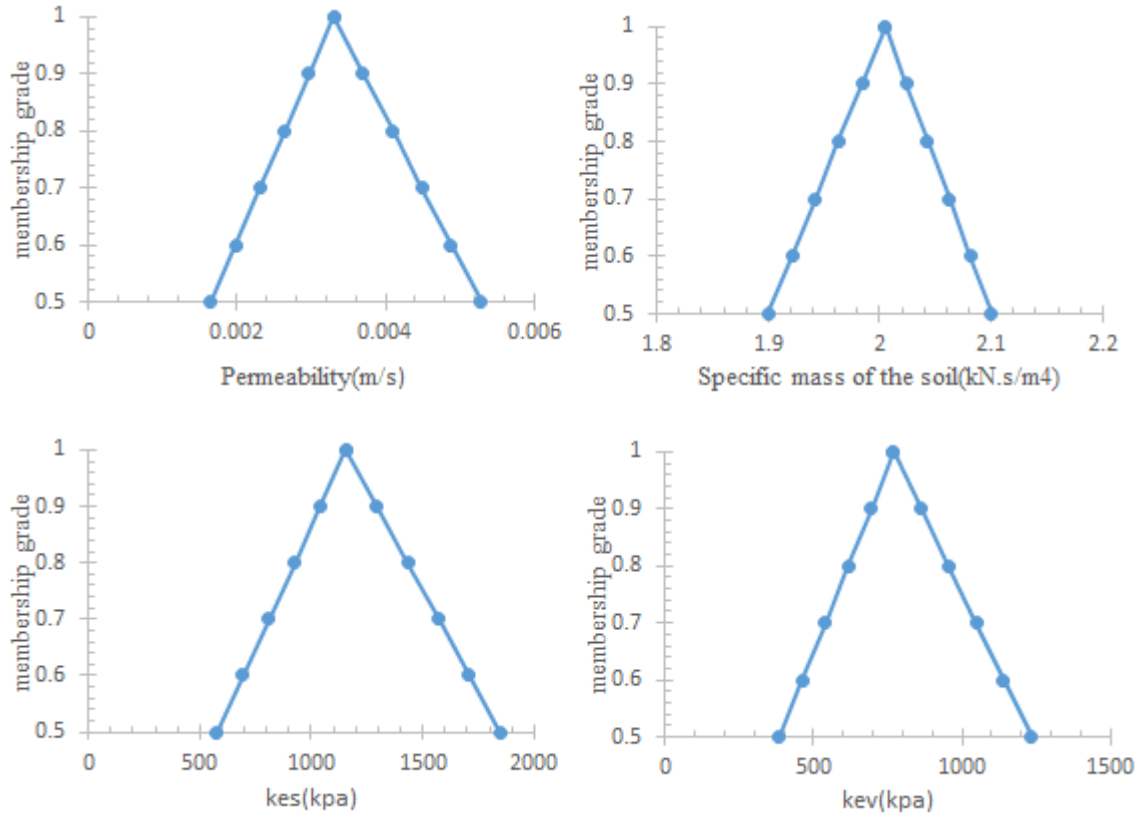


Fig. 4 Membership function of fuzzy input parameters in soil column.

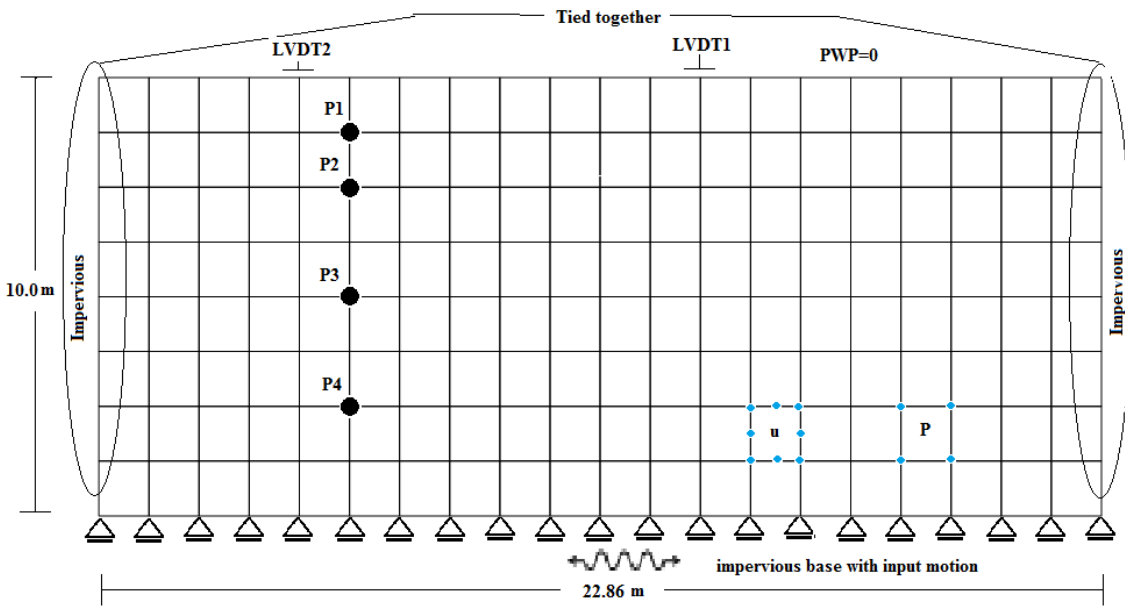
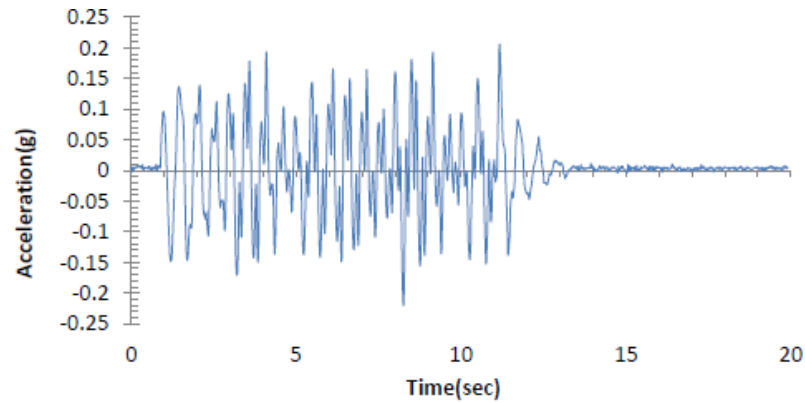


Fig. 5 Finite element mesh used to model the centrifuge test No.1.

Table 2 Location and type of measurement in model No. 1 (Chan et al., 1993).

Measurement	Instrument ID	Depth in prototype scale
pore fluid pressures	P1	1.25 m
pore fluid pressures	P2	2.5 m
pore fluid pressures	P3	5.0 m
pore fluid pressures	P4	7.5 m
vertical displacement	LVDT1	0.0 m
vertical displacement	LVDT2	0.0 m



**Fig. 6** Horizontal input acceleration at the base of the laminar box.

**Table 3** Model parameters of deterministic analysis.

Parameters		Value	Unit
Young's modulus constant	E	990	kPa
Poisson ratio	$\nu$	0.2857	-
Porosity	n	0.42	-
Specific mass of the soil	$\rho_s$	2.005	kN.s/m <sup>4</sup>
Specific mass of the fluid	$\rho_w$	1.0	kN.s/m <sup>4</sup>
permeability coefficient (in model scale)	k	6.6e-5	m/s
permeability coefficient (in prototype scale)	k	3.3e-3	m/s
Volumetric modulus of the solid particle	$k_s$	1.0e17	kPa
Volumetric modulus of the fluid	$k_f$	1.092e6	kPa

**Table 4** Pastor-Zienkiewicz Mark III model parameters of deterministic analysis.

Parameters		Value	Unit
Compressibility modulus at $P'_0$	$K_{ev0}$	770	kPa
Shear modulus at $P'_0$	$K_{es0}$	1155	kPa
Reference pressure $P'_0$	$p'_0$	4	kPa
Critical state line	$M_g$	1.15	-
State line for loading	$M_f$	1.035	-
Dilatancy parameter	$\alpha_g$	0.45	-
Dilatancy parameter	$\alpha_f$	0.45	-
Shear hardening parameter	$\beta_0$	4.2	-
Shear hardening parameter	$\beta_1$	0.2	-
Plastic modulus for loading	$H_0$	600	kPa
Plastic modulus for unloading	$H_{u0}$	4000	kPa
Parameter for plastic unloading	$\gamma_u$	2	-
Parameter for plastic loading	$\gamma_d$	0	-

laminar box is spun at a centrifugal acceleration of 50 g, leading to a prototype soil permeability which is 50 times greater than the permeability of the soil specimen. Therefore, specific permeability is used as an input in equations ( $\frac{k}{\rho_s \hat{G}}$ ) (Tasiopoulou et al., 2015), where  $\hat{G}$  equals to 50 g and  $g$  in the model and prototype scales, respectively. As displayed in Figure 6, the model is simultaneously excited horizontally at the base by the input prototype acceleration. In the current study, the problem was solved in the prototype scale and all the results were demonstrated in the prototype scale. A 2D plane strain model with 160 elements containing 16 solid and 4 fluid degrees of freedom was considered for analyzing the problem, and the side and bottom boundaries of the fluid were taken as impermeable as well. Further, the top of the finite element model acted

as a free boundary, as well as zero pressure for the solid and the fluid phase, respectively. The lateral nodes were fixed together in the finite element model in order to model the resistance of lateral boundary layers.

In other words, the displacement degrees of freedom on the lateral boundary were fixed, ensuring that their movements were identical (Chan, 1988; Rahmani et al., 2012). The static nonlinear analysis was performed to determine the initial stress state of the model. Table 3 represents the parameters used for the Nevada loose sand in this model. Additionally, Pastor-Zienkiewicz Mark III model parameters applied for the constitutive model of the sand during the dynamic loading are provided in Table 4 for the Nevada sand. Since in the present study, an implicit scheme was used for time integration of dynamic

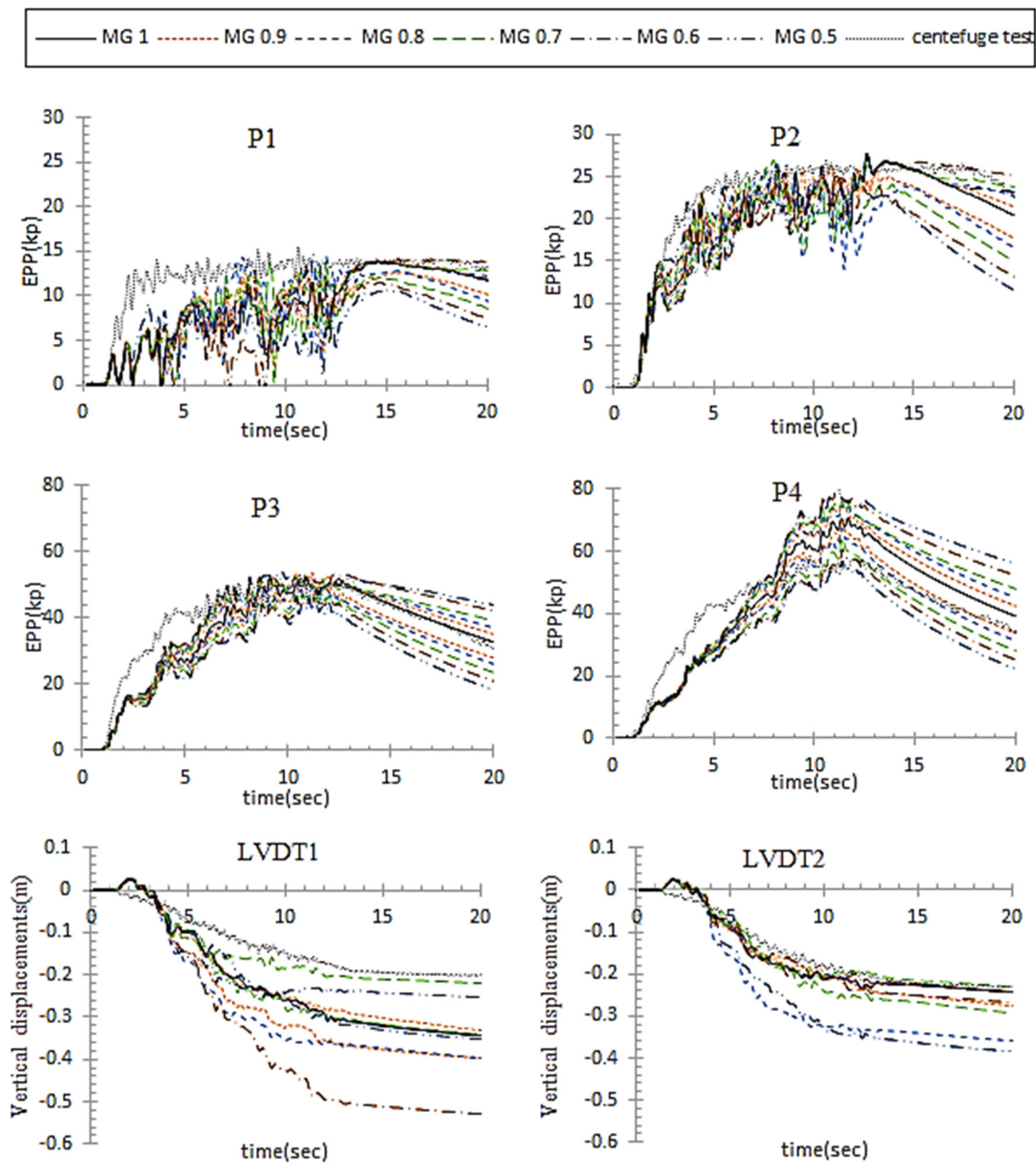


Fig. 7 Excess pore pressure and displacement time history of FFEM model in five membership grades, at different nodes of soil column by assuming  $K$  as an only fuzzy input parameter.

equations, the stability of scheme was independent of the selected time step, and only the accuracy requirements restricted the time step selection. In this respect, the time step used for analysis in this example was 0.0016 sec. The results in membership grade of one were compared with centrifuge experimental results. There was good agreement between numerical and experimental results except in initial times of dynamic analysis which lead to lower excess pore pressures in deep parts (p3, p4). It was interesting that with increasing shear modulus in the solved problem, numerical results were close to experimental results in early times of analysis too.

In the seismic analysis, results depend on the time, so firstly the time history of response was

examined. In this regard, the time histories of the results related to the fuzzification of each single input variable was shown in Figures 7-10 and their cumulative effect, i.e. the effect of considering all these input variables as fuzzy numbers, was shown in Figure 11. It should be noted that, by iterating the proposed scheme to the problem at different  $\alpha$ -cuts, the fuzzy membership function of liquefied soil response is obtained. These membership functions depict that how a assumes liquefied soil response change against the input uncertainties, at what levels are more stable and at what levels are more influenced by uncertainties. According to Figure 7, in the analysis, with the assumption of the permeability coefficient as the only fuzzy input, the fuzzy number

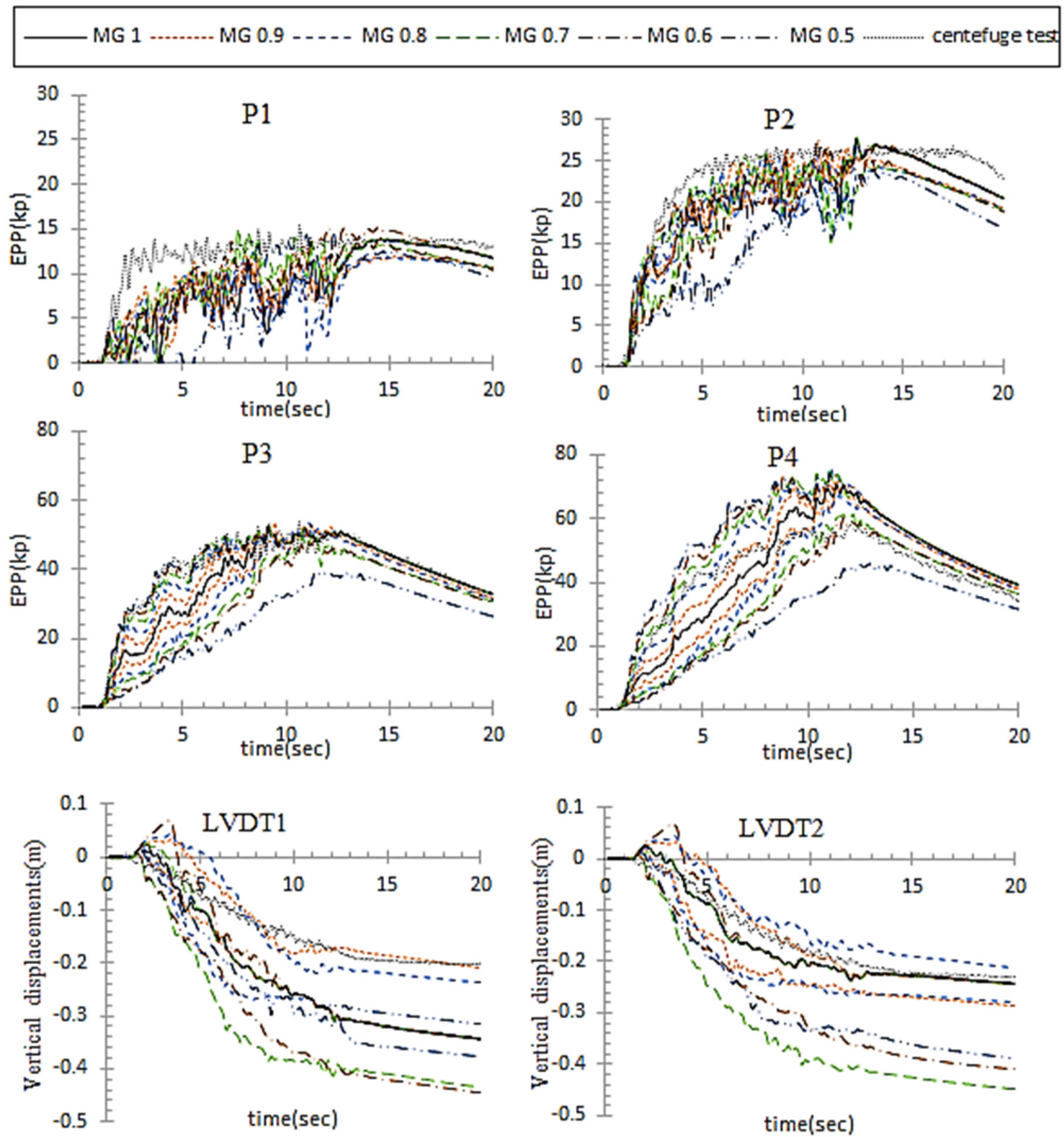


Fig. 8 Excess pore pressure and displacement time history of FFEM model in five membership grades, at different nodes of soil column by assuming  $k_{es}$  as an only fuzzy input parameter.

of the excess pore pressure was increased with depth and time, namely, the support of the corresponding fuzzy number was increased by depth, and the greatest influence of the permeability coefficient was at the deepest point. Also, the effect of changes in permeability coefficient, on the pore pressure value was observed after a delay and its effect was more evident after the end of the earthquake. This delay increased with depth and the reason can be attributed to the drainage distance and time of drainage onset. Adjacent to the free surface (node 1 and partially node 2), drainage was done from the beginning of the loading, but with increase in depth, in early times of earthquake, for the high rate of seismic loading drainage cannot be occur. But over the time this would be possible. Unlike the fluctuations in the results near

the free surface (node 1), the response became more stable and more regular by depth. In the latter case, reducing the permeability coefficient increased the excess pore pressure and vice versa. But, the impact of the permeability increasing on the reduction of pore pressure was greater. After effective time of the earthquake, according to the Figure 7, the effect of increasing the permeability on the percentage of reduction in pore pressure was almost same at all depths. However, the percentage of pore pressure increase caused by the decrease of the permeability coefficient depended on the studying depth. As the depth increased, the relevant percentages increased too. As shown in Figure 8, as  $k_{es}$  assumed as only fuzzy input material parameter, the change in the soil response due to the change in input, increased with

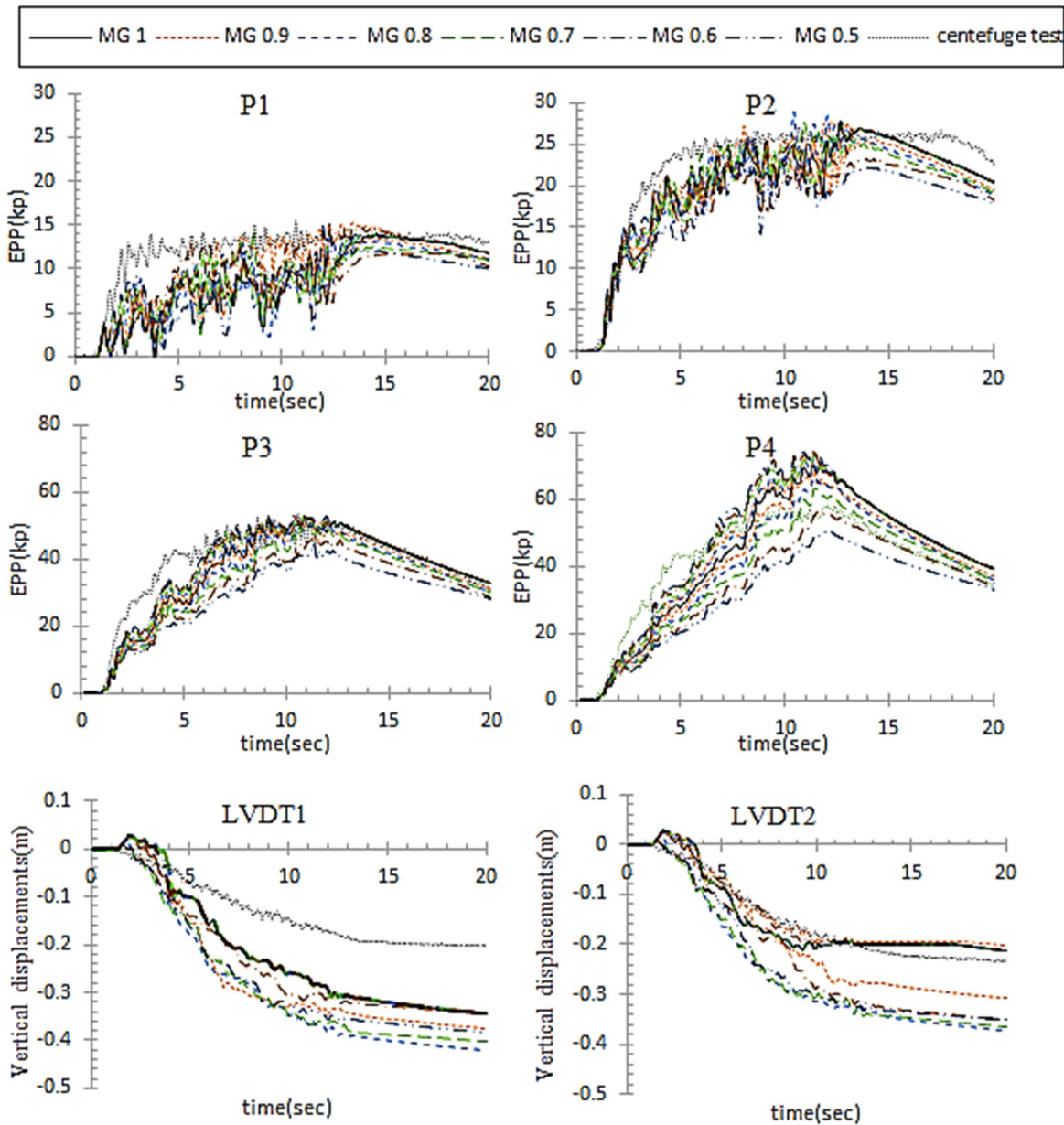


Fig. 9 Excess pore pressure and displacement time history of FFEM model in five membership grades, at different nodes of soil column by assuming  $k_{ev}$  as an only fuzzy input parameter.

depth. The effect of changes in shear modulus was evident on the excess pore pressure from the beginning of the analysis. And after passing the effective time of the earthquake, it became less. According to Figure 9, the pattern of the results in the case of considering the compressibility modulus as an only fuzzy input parameter, was similar to that of the shear modulus one, with this difference that, firstly, changes of results began short time after the earthquake beginning, and secondly, despite the same percentage changes in inputs, the range of changes in the excess pore pressure was lower in this case. As shown in Figure 10, when a specific mass is considered as the only input fuzzy parameter, the support of the fuzzy number of the excess pore pressure was reduced by depth, that was, the greatest effect of the changing in specific mass of the soil, was near the surface and its

effect decreased by increasing the depth. So that about 15 sec after the earthquake begins, the results of the fuzzy analysis converged to the deterministic solution. According to Figure 11, as all four soil material parameters assumes as fuzzy input, the results of the analysis during the effective time of the earthquake were strongly influenced by the shear modulus and partially by compressibility modulus, and after this time, it was mainly affected by the permeability coefficient. The fuzzy method expresses the quantity of these changes with a different level of confidence. Also, it specifies the fluctuation interval of the answer and depending on the importance of the issue, so it will be possible to design and calculate more accurately, without any additional cost. By cross-cutting the time history graph at any given time, the corresponding fuzzy number can be displayed in its usual form. In the

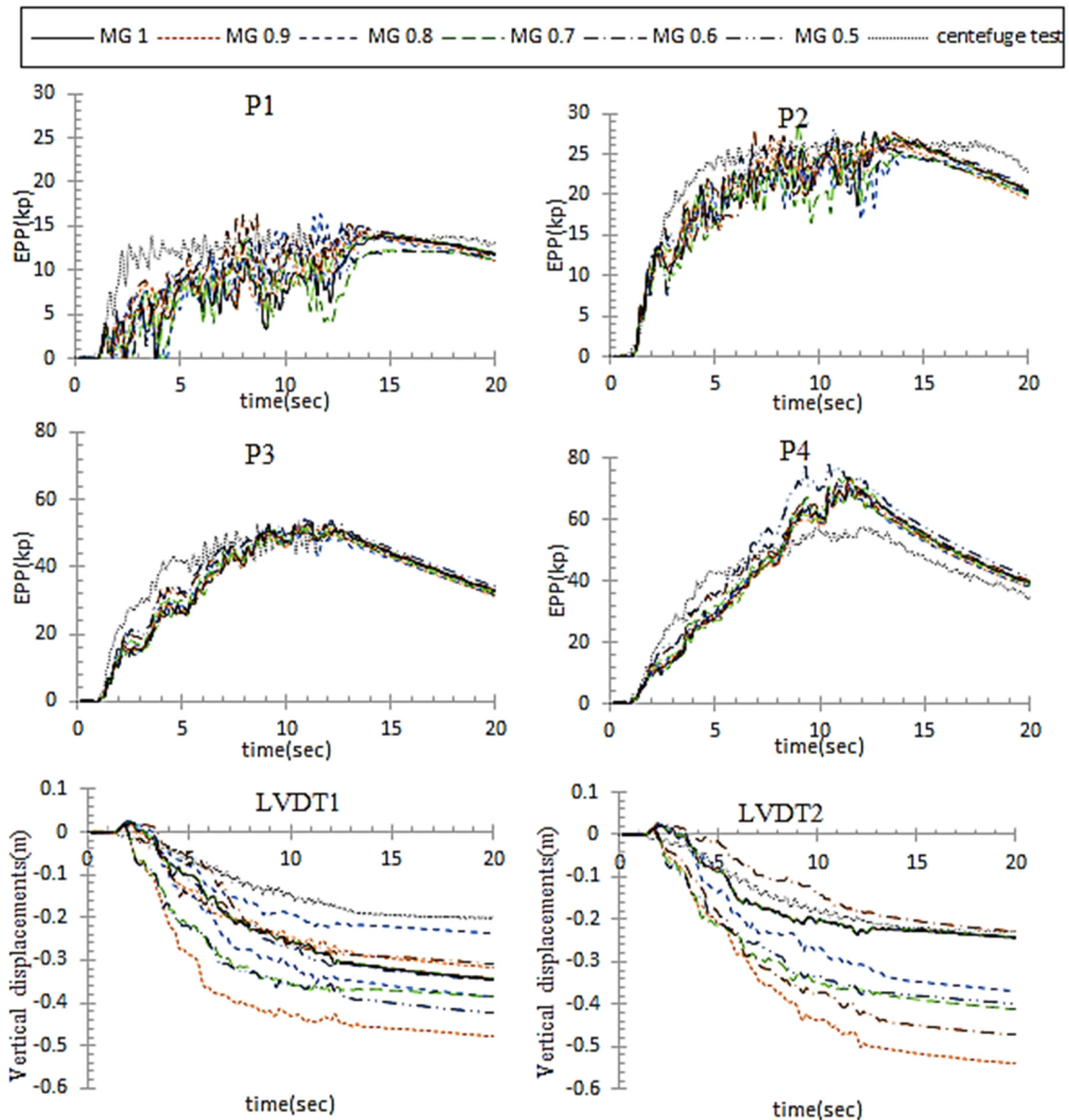


Fig. 10 Excess pore pressure and displacement time history of FFEM model in five membership grades, at different nodes of soil column by assuming  $\rho_s$  as an only fuzzy input parameter.

following, due to the importance of the created maximum excess pore pressure at the onset of the liquefaction, its changes will be discussed in more detail. For this purpose, the percentage of the changes in the response of the model is divided by the percent changes of input parameter, while the other input parameters were kept constant. The results are given in Figures 12-15.

The fuzzy number of the excess pore pressure created over two-time periods of 15 and 20 seconds after the onset of the earthquake was depicted in Figure 16. As can be seen from Figure 16 the linear triangular input fuzzy numbers do not necessarily conclude in linear triangular input fuzzy response; this issue is resulted from the non-linearity of the hydro-mechanical governing equations. Generally,

the focus of uncertainty analysis is on finding the greatest possible uncertainty of the system responses which are associated with support ends at  $\alpha = 0$ , but for better capturing the fuzzy responses nonlinearity the input fuzzy numbers should be discretized by more  $\alpha$  - cuts, in this respect, in the present study five different  $\alpha$  - cuts are considered.

In the following, fuzzy numbers of pore pressure increment (PPI) with fuzzy analysis, which have been compared with deterministic one, were illustrated in Figure 17. Where PPI is defined as:

$$PI(\%) = \frac{EPP_{I_\lambda} - EPP_{Deterministic}}{EPP_{Deterministic}} \times 100 \quad (25)$$

where  $EPP_{I_\lambda}$  and  $EPP_{Deterministic}$  are current pore pressures of fuzzy analysis in the membership grade

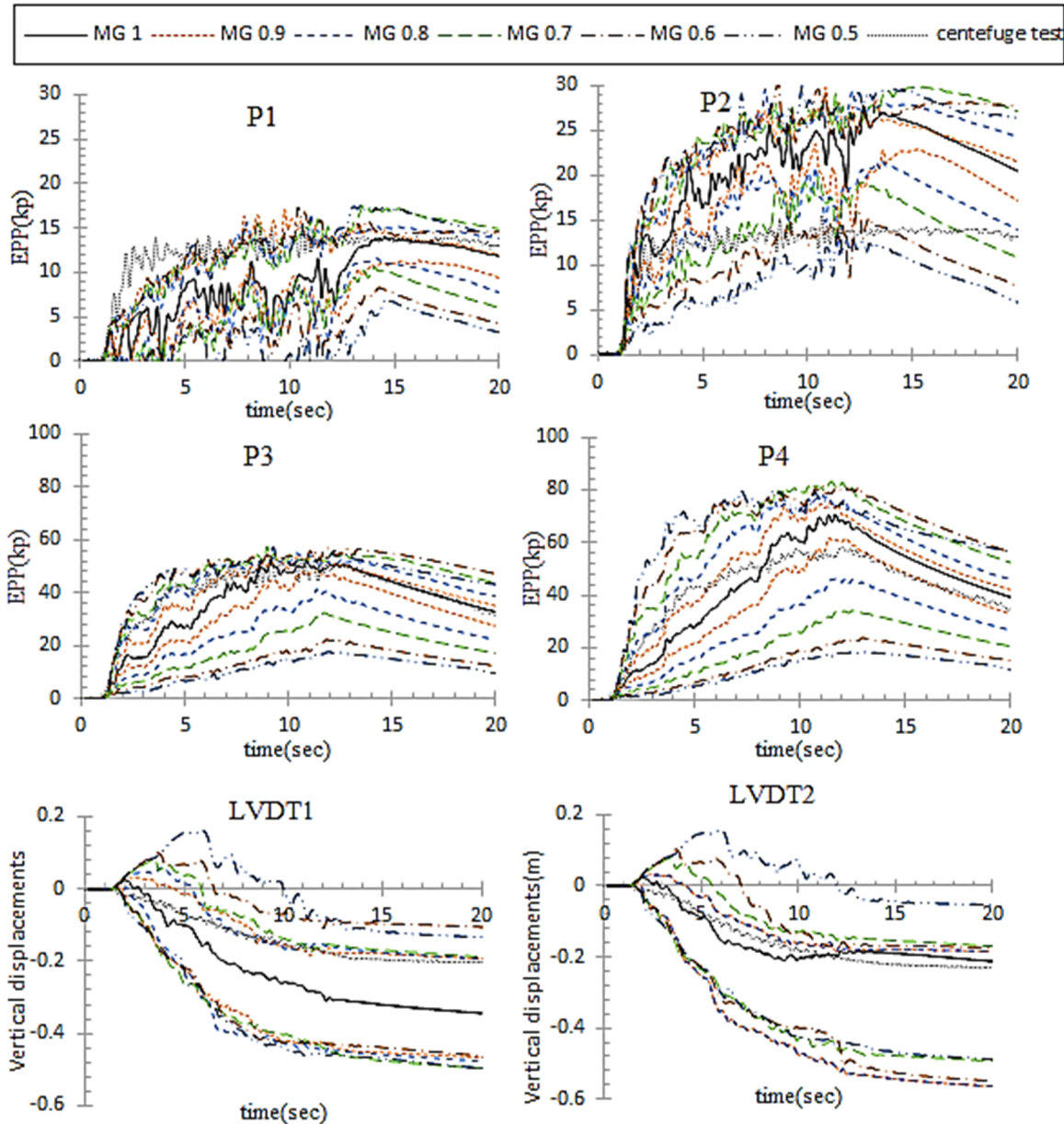


Fig. 11 Excess pore pressure and displacement time history of FFEM model in five membership grades, at different nodes of soil column by assuming ( $K$ ,  $\rho$ ,  $k_{es}$  and  $k_{ev}$ ) as fuzzy input parameters.

of  $\lambda$  and deterministic one, respectively. Also, the fuzzy number of vertical displacements in different depths, 20 seconds after the onset of the earthquake was shown in Figure 18. As shown in this figure, the corresponding fuzzy number on the soil surface had no regular pattern. But it became more regular with increase of depth. So that at depth of 7.5 meters, the most changes were related to the changes in the shear modulus and then, corresponds to the compressibility modulus, permeability coefficient and specific mass of the soil particles, respectively. It should be noted that the percentage of changes in all inputs, excluding specific mass of solid, was same at each membership grade. Changes to the deterministic value, had been increased about 12 % for each membership grade. While this for specific mass of solid was about 6 %.

## CONCLUSIONS

Uncertainty quantification of an engineering problem intends to determine the manner of the input uncertainties would influenced the problem responses and its performance. Such analysis concluded a better understanding of engineering systems design. Using an uncertainty analysis, the system weak points and the parameters with high levels of uncertainty can be identified. In liquefied soil response analysis, considering uncertainties associated with the permeability coefficient, specific mass of the soil, compressibility and shear modulus, affected the soil response, i.e., excess pore water pressure and displacement, and make them uncertain too. Uncertainty in liquefaction analysis may significantly affect the liquefied soil response and intensified the computed results. Present study exploited the fuzzy

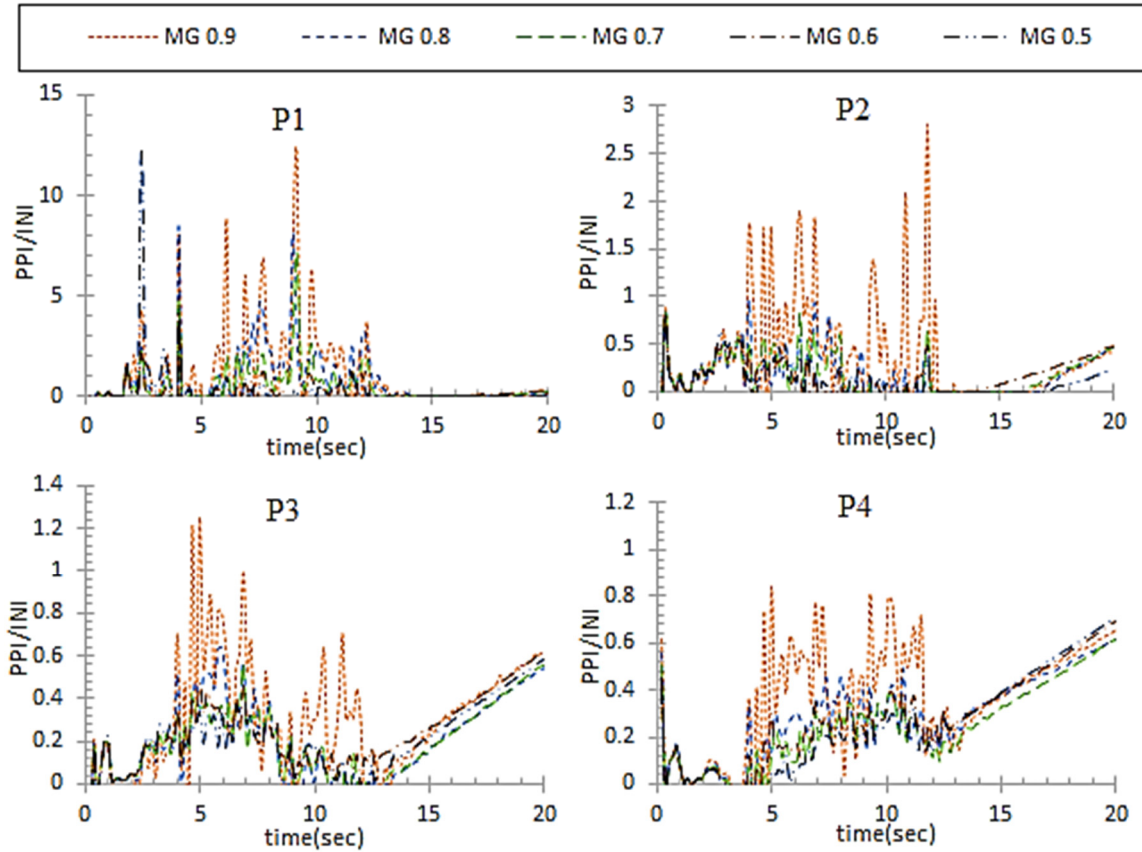


Fig. 12 Excess pore pressure index to percent changes of input parameter history of FFEM model in five membership grades, at different nodes of soil columnby k as the only fuzzy input parameter.

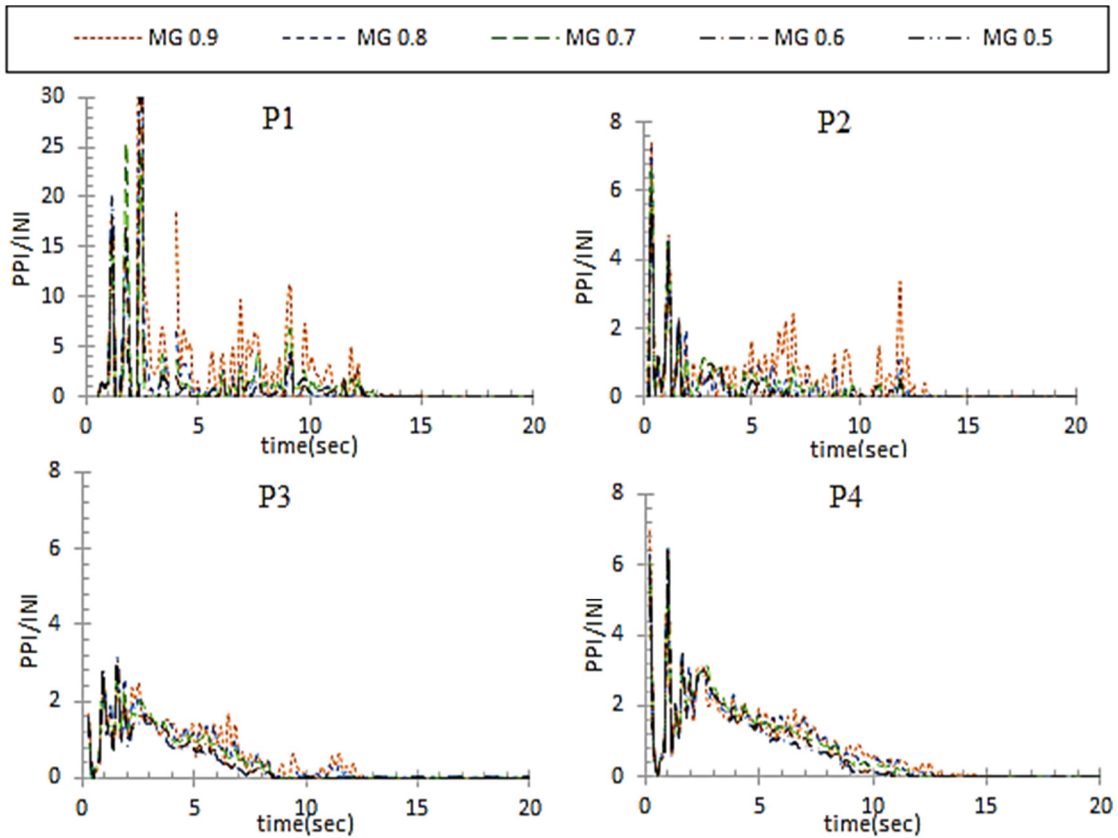


Fig. 13 Excess pore pressure index to percent changes of input parameter history of FFEM model in five membership grades, at different nodes of soil columnby kes as the only fuzzy input parameter.

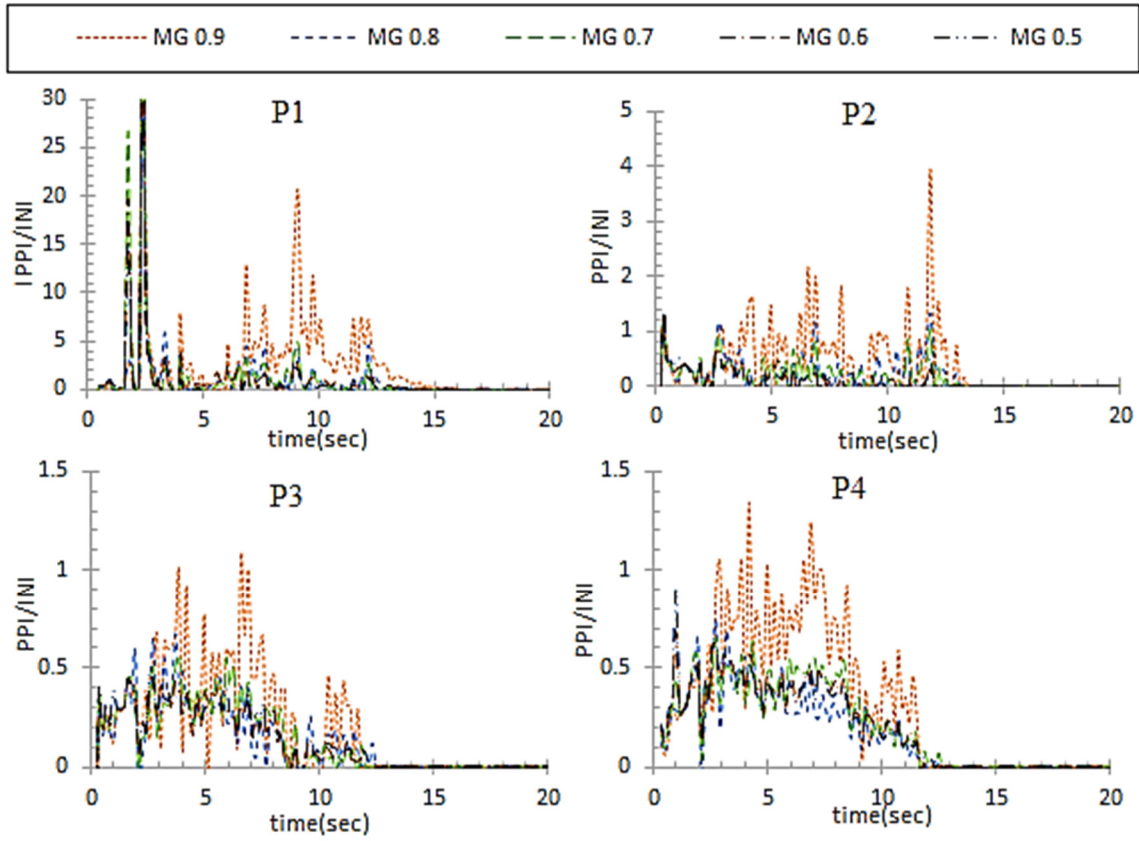


Fig. 14 Excess pore pressure index to percent changes of input parameter history of FFEM model in five membership grades, at different nodes of soil column by  $k_v$  as the only fuzzy input parameter.

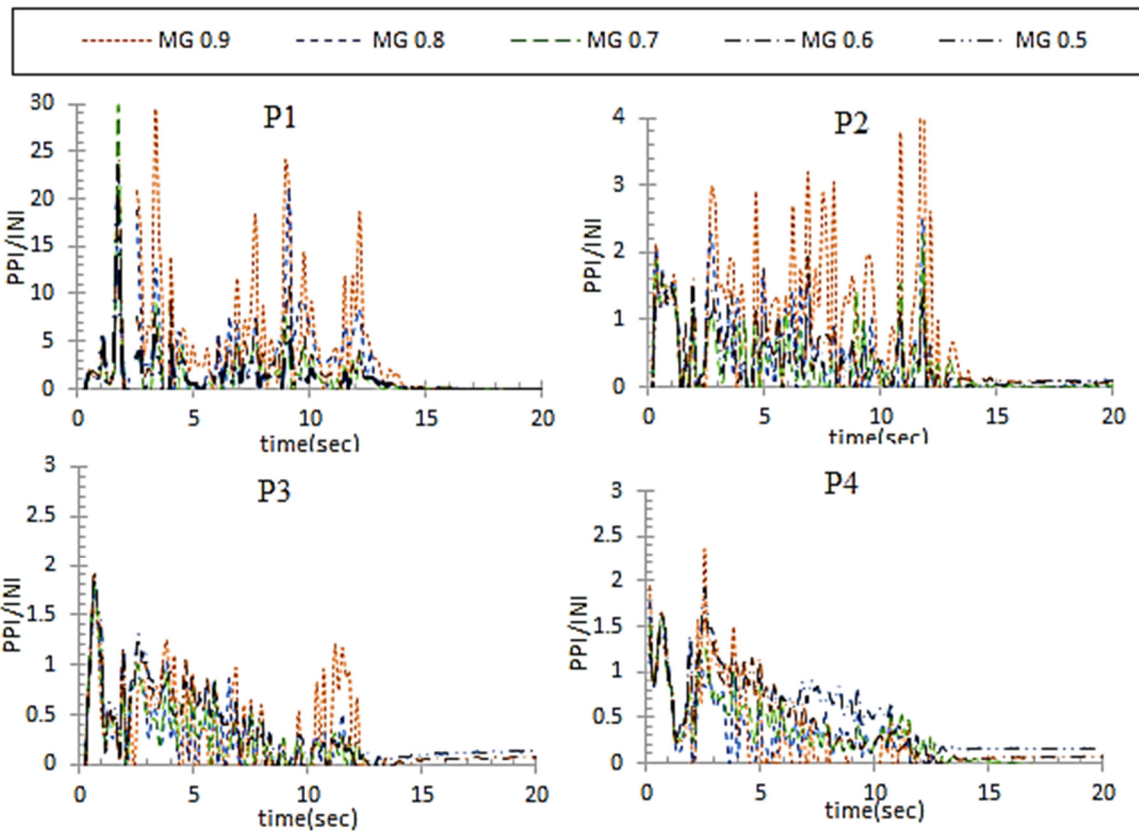


Fig. 15 Excess pore pressure index to percent changes of input parameter history of FFEM model in five membership grades, at different nodes of soil column by  $\rho_s$  as an only fuzzy input parameter.

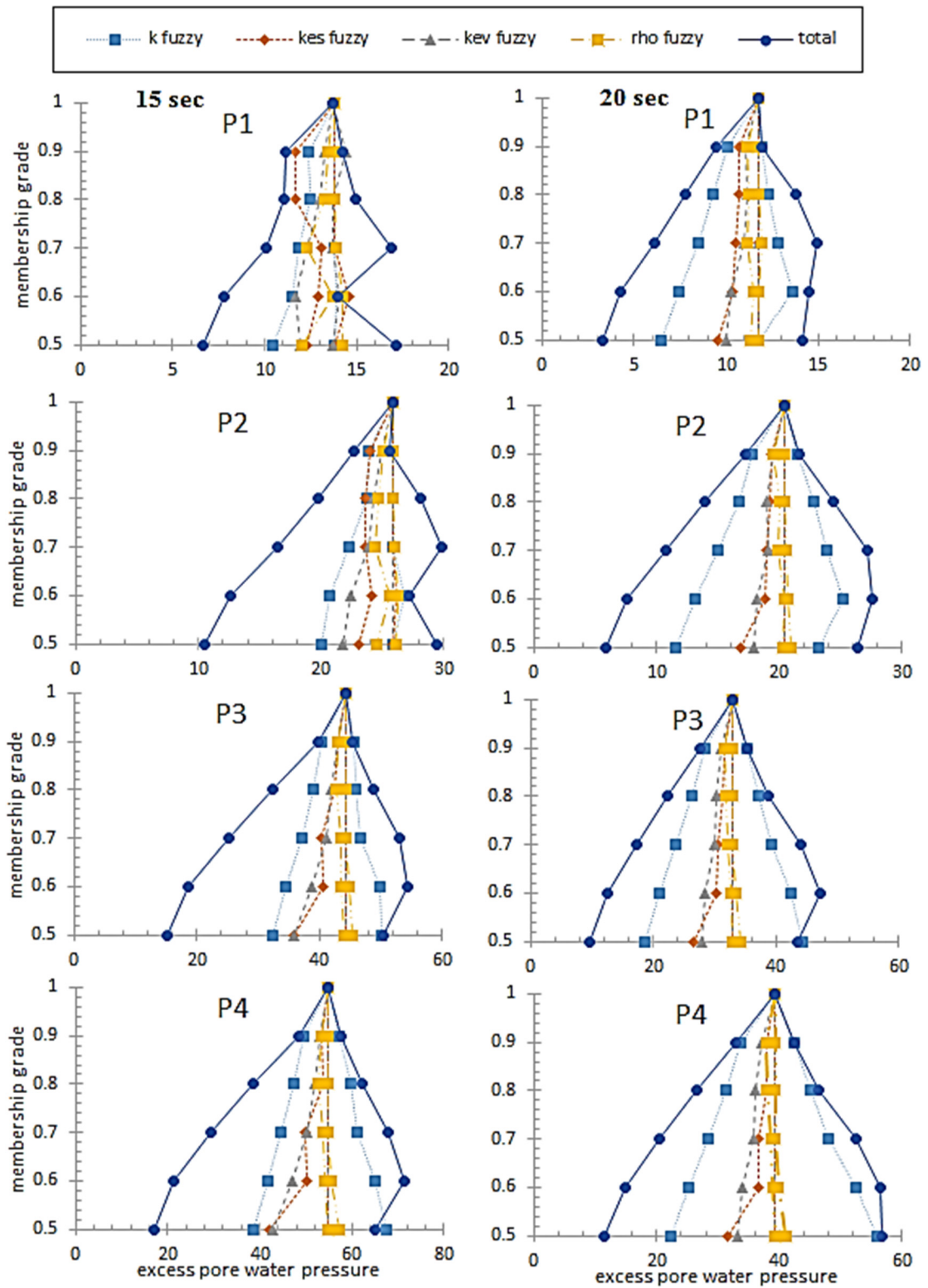


Fig. 16 Fuzzy number of pore pressure in five modes of analysis for different nodes of soil column within 15 and 20 seconds after loading.

sets theory to develop a computational model for uncertainty analysis of soil liquefied. Through an uncertainty analysis, the problem has input parameters that could vary over intervals. Governing hydro-mechanical equations discretized using fuzzy finite element method. In the conventional finite

element method, as a powerful computational method to analysis the complicated problems in geotechnical engineering, such as soil liquefaction during the seismic excitations, the input soil properties are generally imprecise and could not be described with crisp numbers. However, they can be reasonably

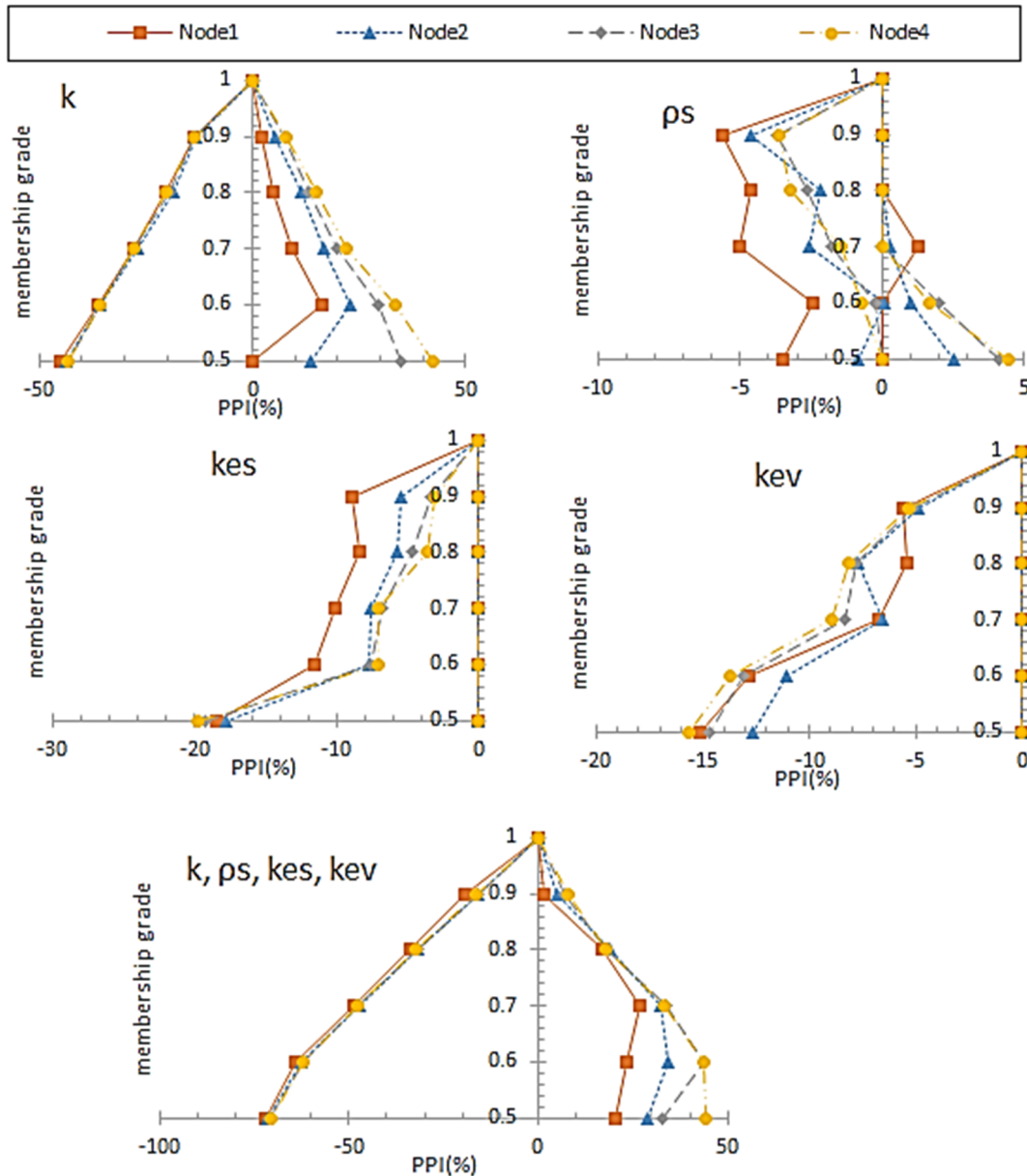
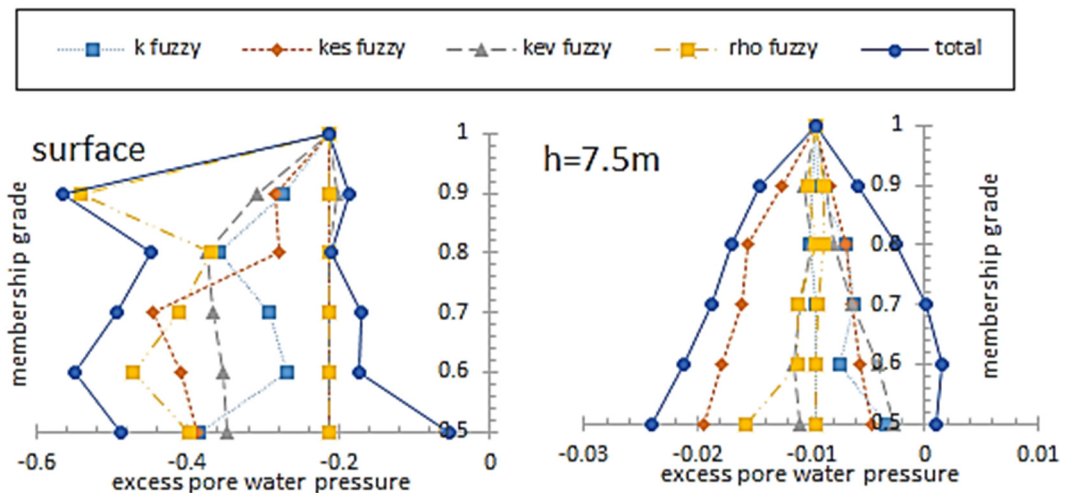


Fig. 17 Fuzzy number of variation percent of pore pressure relative to deterministic solution in five modes of analysis for different nodes of soil column within 20 seconds after loading.

treated as fuzzy numbers to have good estimate about the value of displacements and induced pore pressure during dynamic analysis of porous medium. For this purpose, a fuzzy finite element model (FFEM) has been proposed for analyzing coupled dynamic response of saturated porous medium by treating the soil properties as fuzzy numbers, especially its shear modulus which leads to more reliable answer in deeper points. FFEM make it possible to quantitatively determine how a certain variation in input parameters of the model affects the solution. The results of implementing this approach show that the proposed method is promising. This new modeling framework is suitable for many geotechnical problems where uncertainties are due to insufficient data or imprecise information. One of the distinctive advantages of the fuzzy set approach is the utilization of expert knowledge, which is important for real situations. In

addition to the analysis based on fuzzy parameters, the membership grades can be helpful for the purpose of engineering design. Also, in fuzzy finite element analysis of soils, interaction between soil skeleton and pore water, as a basic principle governing the porous medium, must be considered. Interaction between different domains severely affects the response of soil, especially in dynamic loading and this effect can be depicted in different soil depths by fuzzy finite element method. Since the governing hydro-mechanical equations for soil liquefaction analysis are nonlinear, the responses do not change monotonically with the input uncertainties. As a consequent, for better capturing the fuzzy responses nonlinearity, the input fuzzy numbers should be discretized with smaller  $\alpha$  – cut increments. This, although concluded more accurate fuzzy analysis, significantly increases computations.



**Fig. 18** Fuzzy number of vertical displacement in five modes of analysis for different nodes of soil column within 20 seconds after loading.

#### DATA AVAILABILITY

Some or all data, models, or code generated or used during the study are available from the corresponding author by request, include: developed FORTRAN code, input file of models.

#### ACKNOWLEDGEMENTS

The authors gratefully acknowledge the contributions of Professor Andrew H.C. Chan of the University of Tasmania for providing the computer code (SWANDYNE II) and also for his invaluable comments and guidance.

#### REFERENCES

- Arumoli, K., Muralceetharan, K.K., Hossain, M.M. and Fruth, L.S.: 1992, VELACS (Verification of Liquefaction Analyses by Centrifuge Studies) laboratory testing program: Soil Data Report. The Earth Technology Corporation, NSF, Washington, DC. DOI: 10.13140/2.1.3740.8320
- Biot, M.A.: 1941, General theory of three dimensional consolidation. *Journal of applied physics*, 12(2), 155–164. DOI: 10.1063/1.1712886
- Biot, M.A.: 1956, Theory of propagation of elastic waves in a fluidsaturated porous solid. II. Higher frequency range. *The Journal of the acoustical Society of America*, 28(2), 179–191. DOI: 10.1121/1.1908241
- Biot, M.A.: 1962, Mechanics of deformation and acoustic propagation in porous media. *Journal of applied physics*, 33(4), 1482–1498. DOI: 10.1063/1.1728759
- Chan, A.H.-C.: 1988, A unified finite element solution to static and dynamic problems of geomechanics. Swansea University.
- Chan, A.H.C., Famiyesin, O. and Muir Wood, D.: 1993, Numerical Prediction for Model No. 1, In *Verification of numerical procedures for the analysis of soil liquefaction problems*, K. Arulanandan and R.F. Scott, Eds. International Conference on the Verification of Numerical Procedures for the Analysis of Soil Liquefaction Problems (Davis, Calif.). AA Balkema.
- Cen, W.J., Luo, J.R., Zhang, W.D. and Rahman, M.S.: 2018, An Enhanced Generalized Plasticity Model for Coarse Granular Material considering Particle Breakage. *Advances in Civil Engineering*. DOI: 10.1155/2018/7242936
- Dong, W. and Shah, H.C.: 1987, Vertex method for computing functions of fuzzy variables. *Fuzzy sets and Systems*, 24(1), 65–78. DOI: 10.1016/0165-0114(87)90114-X
- Dong, W., Shah, H. and Wongt, F.: 1985, Fuzzy computations in risk and decision analysis. *Civil Engineering Systems*, 2(4), 201–208. DOI: 10.1080/02630258508970407
- Faes, M., Cerneels, J., Vandepitte, D. and Moens, D.: 2017, Identification and quantification of multivariate interval uncertainty in finite element models. *Computer Methods in applied mechanics and engineering*, 315, 896–920. DOI: 10.1016/j.cma.2016.11.023
- Farkas, L., Moens, D., Vandepitte, D. and Desmet, W.: 2010, Fuzzy finite element analysis based on reanalysis technique. *Structural Safety*, 32(6), 442–448. DOI: 10.1016/j.strusafe.2010.04.004
- Faybishenko, B.: 2010, Fuzzy-probabilistic calculations of water-balance uncertainty. *Stochastic Environmental Research and Risk Assessment*, 24(6), 939–952. DOI: 10.1007/s00477-010-0379-y
- Fenton, G.A.: 1990, Simulation and analysis of random fields. PhD thesis, Princeton University.
- Fenton, G.A. and Griffith, D.V.: 2008, Risk assessment in Geotechnical Engineering. Johan Wiley & Sons, Inc.
- Hosseinejad, F. and Kalateh, F.: 2017, Using Fuzzy FEM in Dynamic Coupled Analysis of Saturated Porous Media. *Modares Civil Engineering journal*, 17(5), 193–206.
- Hosseinejad, F., Kalateh, F. and Mojtahedi, A.: 2019, Numerical Investigation of liquefaction in earth dams: A Comparison of Darcy and Non-Darcy flow models. *Computers and Geotechnics*, 116, 103182. DOI: 10.1016/j.compgeo.2019.103182
- Khoei, A., Anahid, M., Zarinfar, M., Ashouri, M. and Pak, A.: 2011a, A large plasticity deformation of unsaturated soil for 3D dynamic analysis of lower sanfernando dam. *Asian Journal of Civil Engineering (Building and Housing)*, 12(1), 1–25.
- Khoei, A., Azami, A. and Haeri, S.: 2004, Implementation of plasticity based models in dynamic analysis of earth

- and rockfill dams: A comparison of Pastor–Zienkiewicz and cap models. *Computers and Geotechnics*, 31(5), 384–409.  
DOI: 10.1016/j.compgeo.2004.04.003
- Khoei, A. and Mohammadnejad, T.: 2011b, Numerical modeling of multiphase fluid flow in deforming porous media: A comparison between two-and three-phase models for seismic analysis of earth and rockfill dams. *Computers and Geotechnics*, 38(2), 142–166.  
DOI: 10.1016/j.compgeo.2010.10.010
- Li, K. and Lumb, P.: 1987, Probabilistic design of slopes. *Canadian Geotechnical Journal*, 24(4), 520–535.  
DOI: 10.1139/t87-068
- McBratney, A.B. and Odeh, I.O.: 1997, Application of fuzzy sets in soil science: fuzzy logic, fuzzy measurements and fuzzy decisions. *Geoderma*, 77(2-4), 85–113.  
DOI: 10.1016/S0016-7061(97)00017-7
- Meidani, M., Habibagahi, G. and Katebi, S.: 2004, An aggregated fuzzy reliability index for slope stability analysis. *Iranian Journal of Fuzzy Systems*, 1(1), 17–31.
- Mira, P., Tonni, L., Pastor, M. and Fernández Merodo, J.A., 2009, A generalized midpoint algorithm for the integration of a generalized plasticity model for sands. *International journal for numerical methods in engineering*, 77(9), 1201–1223.  
DOI: 10.1002/nme.2445
- Moens, D. and Hanss, M.: 2011, Non-probabilistic finite element analysis for parametric uncertainty treatment in applied mechanics: Recent advances. *Finite Elements in Analysis and Design*, 47(1), 4–16.  
DOI: 10.1016/j.finel.2010.07.010
- Mroz, Z. and Zienkiewicz, O.C.: 1984, Uniform formulation of constitutive equations for clays and sand. In: *Mechanics of engineering materials*, Desai CS, Gallagher RH (eds) Chapter 22, Wiley, New York, 415–459.
- Ohtomo, K. and Shinozuka, M.: 1990, Two-dimensional spatial severity of liquefaction. *Proc. 8th Japan Earthquake Engng Symp.*, Tokyo, 123–128.
- Pastor, M., Zienkiewicz, O. and Chan, A.: 1990, Generalized plasticity and the modelling of soil behaviour. *International Journal for Numerical and Analytical Methods in Geomechanics*, 14(3), 151–190.  
DOI: 10.1002/nag.1610140302
- Popescu, R. and Prevost, J.H.: 1995, Comparison between VELACS numerical 'class A' predictions and centrifuge experimental soil test results. *Soil Dynamics and Earthquake Engng.*, 14(2), 79–92.  
DOI: 10.1016/0267-7261(94)00038-1
- Popescu, R., Prevost, J.H. and Deodatis, G.: 1997, Effects of spatial variability on soil liquefaction: some design recommendations, *Geotechnique*, 47(5), 1019–1036.  
DOI: 10.1680/geot.1997.47.5.1019
- Rahmani, A., Fare, O.G., and Pak, A.: 2012, Investigation of the influence of permeability coefficient on the numerical modeling of the liquefaction phenomenon. *Scientia Iranica*, 19(2), 179–187.  
DOI: 10.1016/j.scient.2012.02.010
- Ross, T.J.: 2004, *Fuzzy logic with engineering applications*. Vol. 2., Wiley Online Library.
- Sadeghian, S. and Namin, M.L.: 2013, Using state parameter to improve numerical prediction of a generalized plasticity constitutive model. *Computers & geosciences*, 51, 255–268. DOI: 10.1016/j.cageo.2012.06.025
- Silva, A.V., Neto, S.A.D. and de Sousa Filho, F.D.A.: 2016, A Simplified Method for Risk Assessment in Slope Stability Analysis of Earth Dams Using Fuzzy Numbers. *Electronic Journal of Geotechnical Engineering*, 21(10), 3607–3624.
- Taboada, V.M. and Dobry, R.: 1993, Experimental results of model no. p. 1 at RPI, In *Verification of numerical procedures for the analysis of soil liquefaction problems*, K. Arulanandan and R.F. Scott, Eds. in *International Conference on the Verification of Numerical Procedures for the Analysis of Soil Liquefaction Problems (1993: Davis, Calif.)*. AA Balkema.
- Tamayo, J.L.P. and Awruch, A.M.: 2016, On the validation of a numerical model for the analysis of soil-structure interaction problems. *Latin American Journal of Solids and Structures*, 13(8), 1545–1575.  
DOI: 10.1590/1679-78252450
- Tasiopoulou, P., Taiebat, M., Tafazzoli, N. and Jeremić, B.: 2015, On validation of fully coupled behavior of porous media using centrifuge test results. *Coupled systems mechanics*, 4(1), 37–65.  
DOI: 10.12989/csm.2015.4.1.037
- Taslimian, R.: 2013, *Numerical simulation of liquefaction in non-darcy saturated porous media with irregular layers*. University of Tehran, Thesis, Chapter 4, (in Persian).
- Ural, D.: 1995, *The effects of spatial variability of soil properties on liquefaction*. PhD thesis, Princeton University.
- Valliappan, S. and Pham, T.: 1993, Fuzzy finite element analysis of a foundation on an elastic soil medium. *International journal for numerical and analytical methods in geomechanics*, 17(11), 771–789.  
DOI: 10.1002/nag.1610171103
- Valliappan, S. and Pham, T.: 1995, Elasto-plastic finite element analysis with fuzzy parameters. *International Journal for Numerical Methods in Engineering*, 38(4), 531–548. DOI: 10.1002/nme.1620380403
- Ye, J., Jeng, D., Wang, R. and Zhu, C.: 2013, Validation of a 2-D semi-coupled numerical model for fluid–structure–seabed interaction. *Journal of Fluids and Structures*, 42, 333–357.  
DOI: 10.1016/j.jfluidstructs.2013.04.008
- Zadeh, L.A.: 1999, Fuzzy sets as a basis for a theory of possibility. *Fuzzy sets and systems*, 100, 9–34.  
DOI: 10.1016/S0165-0114(99)80004-9
- Zienkiewicz, O. and Bettess, P.: 1982, *Soils and other saturated media under transient, dynamic load conditions*. Soil Mechanics Transient and Cyclic Loads, Pande & Zienkiewicz eds. John Wiley and Sons.
- Zienkiewicz, O.C., Chan, A.H.C., Pastor, M., Paul, D.K. and Shiomi, T.: 1990, Static and dynamic behaviour of soils: a rational approach to quantitative solutions. I. Fully saturated problems. *Proceedings of the Royal Society of London. A. Mathematical and Physical Sciences*, 429(1877), 285–309.  
DOI: 10.1098/rspa.1990.0061
- Zienkiewicz, O.C., Chan, A.H.C., Pastor, M., Schrefler, B.A. and Shiomi, T.: 1999, *Computational geomechanics*. John Wiley & Sons, Citeseer.
- Zienkiewicz, O. and Shiomi, T.: 1984, Dynamic behaviour of saturated porous media; the generalized Biot formulation and its numerical solution. *International journal for numerical and analytical methods in geomechanics*, 8(1), 71–96.  
DOI: 10.1002/nag.1610080106

## APPENDIX A: PASTRO–ZIENKIEWICZ CONSTITUTIVE SOIL MODEL

In the general plasticity method (Mroz and Zienkiewicz, 1984; Pastor et al., 1990), no yielding or plastic potential surface is explicitly defined while their derivatives are only used. Further, in general plasticity, plastic deformation is possible at any strain level regardless of the direction of stress increase (i.e. in both loading and unloading conditions). Furthermore, the elasto-plastic behaviour of materials is described by the following incremental relation between stress and strain components.

$$d\sigma = D: d\varepsilon \quad (\text{A1})$$

where  $d\varepsilon$  is the strain component containing elastic (e) and plastic (p) parts. It should be noted that the stress component ( $d\sigma$ ) of the elastic and plastic parts is the same (Taslimian, 2013)

$$d\varepsilon = d\varepsilon^e + d\varepsilon^p \quad (\text{A2})$$

$$d\sigma = D^e: d\varepsilon^e \quad (\text{A3})$$

$$d\sigma = D^p: d\varepsilon^p \quad (\text{A4})$$

Loading or unloading conditions should be specified due to the dependence of  $D$  on the stress path. If  $n_g$  is considered as the unit vector, which is normal to stress increment, then the loading and unloading conditions are defined as follows:

$$n_g: ds^e > 0 \quad \text{Loading} \quad (\text{A5})$$

$$n_g: ds^e < 0 \quad \text{UnLoading} \quad (\text{A6})$$

$$n_g: ds^e = 0 \quad \text{Neutral} \quad (\text{A7})$$

where  $d\sigma^e$  denotes the elastic stress increment and is observed when the behaviour of materials is completely elastic. Additionally, the neutral state is regarded as a limit state and is related to the reversible stress increment. Depending on the loading or unloading conditions, two modes are available for the elasto-plastic tangent matrix. To satisfy the continuity condition, it is defined as follows:

$$D_{L/U}^{-1} = (D^e)^{-1} d\varepsilon + \frac{1}{H_{L/U}} [m_{L/U} \otimes n_g] \quad (\text{A8})$$

where  $m_L$  and  $m_U$  are the unit vectors and represent plastic flow direction during the loading and unloading conditions, respectively. In addition,  $H_L$  and  $H_U$  are the scalar quantities that demonstrate the plastic modulus functions in loading and unloading conditions, respectively. Finally,  $D^e$  denotes the elastic tangent matrix. The hardening modules and plastic flow directions can be determined without referring to the yield and the plastic potential function, and specifying the increased stress relies on the loading or unloading direction. Therefore, these two different conditions can be defined by various terms. Further, the continuity parameter is expressed as follows:

$$d\lambda = \frac{n_g: D^e: d\varepsilon}{H_{L/U} + n_g: D^e: m_{L/U}} \quad (\text{A9})$$

More importantly, although the yield and potential functions are not explicitly defined, they can be obtained by integrating the  $m_{U/L}$ ,  $n_g$  vectors. Pastor–Zienkiewicz Mark III model, as a special case of general plasticity, is developed to predict the behaviour of granular soils under monotonic and cyclic loading. In this model, the problem solution is assumed isotropic, and constitutive equations are written in terms of the stress invariants  $\dot{p}$ ,  $q$  and  $\theta$  as

$$\dot{p} = \frac{1}{3} I: \sigma = \frac{1}{3} \text{tr}(\sigma) = \frac{1}{3} \sigma_{kk} \quad (\text{A10})$$

$$q = \sqrt{3j_2} \quad (\text{A11})$$

$$\theta = \frac{1}{3} \sin^{-1} \left( -\frac{3\sqrt{3}}{2} \cdot \frac{j_3}{j_2^{3/2}} \right) \quad (\text{A12})$$

The nature of the sand behaviour should be studied in the laboratory for its modelling, and finding the soil dilatancy is regarded as the first step in this aspect.

$$d_g = \frac{d\varepsilon_p}{d\varepsilon_q} \quad (\text{A13})$$

where  $d\varepsilon_p$  and  $d\varepsilon_q$  are volumetric and shear strains, respectively. From the experiments conducted on the sand, the

amount of dilatancy ( $d_g$ ) is independent of the stress component amount and its direction for a constant stress point in space of the stress invariants, and thus, it can be approached by a linear function of the stress ratio,  $\eta = q/\hat{p}$ . Therefore, soil dilatation is defined as a function of the ratio of the mean stress to deviatoric stress as follows:

$$d_g = (1 + \alpha_g) \cdot (M_g - \eta) \quad (\text{A14})$$

where  $\alpha_g$  and  $M_g$  represent the aggregate parameter and the gradient of the critical state line in the  $\hat{p}$ - $q$  plane. If  $\phi_g$  is the remaining friction angle in the tri-axial test, by generalising the  $M_g$  to three-dimensional stress conditions through modifying the Mohr–Coulomb type, we obtain

$$M_g = \frac{6 \sin \phi_g}{3 - \sin \phi_g \cdot \sin 3\theta} \quad (\text{A15})$$

Therefore, the components of plastic flow vector in loading conditions ( $\mathbf{m}_L$ ) are defined on the main stresses space as follows:

$$m_{L,v} = \frac{d_g}{\sqrt{1+d_g^2}} \quad (\text{A16})$$

$$m_{L,s} = \frac{1}{\sqrt{1+d_g^2}} \quad (\text{A17})$$

$$m_{L,\theta} = -\frac{qM_g \cos 3\theta}{2\sqrt{1+d_g^2}} \quad (\text{A18})$$

To transfer to the Cartesian space, multiplying the  $\mathbf{m}_L$  components in the base vectors is necessary. Such components are derivative of the stress invariants relative to the stress  $\sigma$ .

$$\mathbf{m}_L = m_{L,v} \cdot \frac{d\hat{p}}{d\sigma} + m_{L,s} \cdot \frac{dq}{d\sigma} + m_{L,\theta} \cdot \frac{d\theta}{d\sigma} \quad (\text{A19})$$

Furthermore, the irreversible strain is contractile for the loading mode. Therefore, the  $\mathbf{m}_u$  components are defined as

$$m_{U,v} = -\text{abs}(m_{L,v}) \quad (\text{A20})$$

$$m_{U,s} = m_{L,s} \quad (\text{A21})$$

$$m_{U,\theta} = m_{L,\theta} \quad (\text{A22})$$

The loading direction ( $\mathbf{n}_g$ ) varies from the potential flow direction ( $\mathbf{m}$ ), as non-associated flow rule is assumed in this model. However, they are defined by similar terms as follows:

$$\mathbf{n}_v = \frac{d_f}{\sqrt{1+d_f^2}} \quad (\text{A23})$$

$$\mathbf{n}_s = \frac{1}{\sqrt{1+d_f^2}} \quad (\text{A24})$$

$$\mathbf{n}_\theta = -\frac{qM_f \cos 3\theta}{2\sqrt{1+d_f^2}} \quad (\text{A25})$$

$$d_f = (1 + \alpha_f) \cdot (M_f - \eta) \quad (\text{A26})$$

where  $\alpha_f$  and  $M_f$  are model parameters. The hardness reduces and the material condition approximates the critical condition by increasing shear plastic deformation, which is the characteristic behaviour of the sands. By considering  $H_L$  as the plastic modulus in loading, Pastor et al. (1990) formulated this fact as follows:

$$H_L = H_0 \cdot \hat{p} \cdot H_f \cdot \{H_v + H_s\} H_{DM} \quad (\text{A27})$$

$$H_f = \left(1 - \frac{\eta}{M_f} \cdot \frac{\alpha_f}{1+\alpha_f}\right)^4 \quad (\text{A28})$$

$$H_v = 1 - \frac{\eta}{M_g} \quad (\text{A29})$$

$$H_s = \beta_0 \cdot \beta_1 \cdot \exp(-\beta_0 \xi) \quad (\text{A30})$$

$$H_{DM} = \left(\frac{\zeta_{max}}{\zeta}\right)^{\gamma_d} \quad (\text{A31})$$

$$\xi = \int |d\epsilon_s^p| = \int d\xi \quad (\text{A32})$$

$$\zeta = \dot{p} \left\{ 1 - \left( \frac{\alpha_f}{1+\alpha_f} \right) \cdot \frac{\eta}{M_f} \right\}^{-1/\alpha_f} \quad (\text{A33})$$

where  $H_0, \beta_0, \beta_1$  and  $\gamma_d$  are model parameters and  $\xi$  denotes the cumulative deviatoric plastic strain. Additionally,  $\zeta$  and  $\zeta_{max}$  represent the mobilised stress function and the maximum value previously reached by the mobilised stress function. The plastic modulus obtained from Eq. (A27) can model some of the characteristics of the behaviour of the granular soils such as the rupture in critical condition, the softness of the sands and non-swelling (dilatation) of the loose sand. In the case of unloading, the plastic modulus ( $H_U$ ) is defined as

$$H_U = H_{u0} \left(\frac{M_g}{\eta_u}\right)^{\gamma_u} \text{ for } \left|\frac{M_g}{\eta_u}\right| > 1 \quad (\text{A34})$$

$$H_U = H_{u0} \text{ for } \left|\frac{M_g}{\eta_u}\right| \leq 1 \quad (\text{A35})$$

where  $H_{u0}$  and  $\gamma_u$  indicate the model parameters and  $\eta_u$  is the stress ratio at which the unloading occurs. In the Pastor–Zienkiewicz model, the soil is assumed to have a non-linear elastic response and the reversible non-linear behaviour is expressed by a hypo-elastic approach, in which the bulk and shear modulus only rely on the hydrostatic pressure and are expressed as follows:

$$K_{ev} = K_{ev0} \frac{\dot{p}}{\dot{p}_0} \quad (\text{A36})$$

$$G = G_0 \frac{\dot{p}}{\dot{p}_0} \quad (\text{A37})$$

where  $\dot{p}_{0,b}$  is the hydrostatic pressure when the model parameters are measured, and  $K_{ev0}$  and  $G_0 = k_{es0}/3$  represent the initial values of the shear and bulk modulus, respectively.